Non-perennial stream networks as directed acyclic graphs: The R-package streamDAG

Ken Aho[1*], Cathy Kriloff[2], Sarah E. Godsey[3], Rob Ramos[4], Chris Wheeler[5], Yaqi You[6], Sara Warix[3], DeWayne Derryberry[2], Sam Zipper[5], Rebecca L.Hale[7]

[1]Department of Biological Sciences, Idaho State University, Pocatello, ID 83209-8007, *Corresponding author (ahoken@isu.edu; 1-208-282-3391)

[2]Department of Mathematics and Statistics, Idaho State University, Pocatello, ID 83209-8085

[3]Department of Geosciences, Idaho State University, Pocatello, ID 83209-8072

[4]Division of Biology, Kansas State University, Manhattan, KS 66506

[5]Kansas Geological Survey, The University of Kansas, Lawrence, KS 66047-3724

[6]Department of Environmental Resources Engineering, The State University of New York, College of Environmental Science and Forestry, Syracuse, NY 13210

[7]Smithsonian Environmental Research Center, Edgewater, MD 21037

This paper is a non-peer reviewed preprint submitted to EarthArXiv. The paper will be submitted for peer review to the journal *Environmental Modelling and Software*

Abstract

Many conventional stream network metrics are time-invariant and/or do not consider the importance of individual stream locations to network functionality. As a result, they are not well-suited to non-perennial streams, in which hydrologic status (flowing vs. pooled vs. dry) can vary substantially in space and time. To help address this issue, we consider non-perennial streams as directed acyclic graphs (DAGs). DAG metrics allow: 1) summarization of important network characteristics (e.g., centrality, complexity, connectedness, and nestedness) of both particular (local) stream network locations and entire (global) stream networks, and 2) tracking of these characteristics as non-perennial stream networks expand and shrink. We review a large number of graph-theoretic procedures for their utility in the analysis of non-perennial stream DAGs. Approaches we find useful are codified in a new publicly available **R**-package, *streamDAG*, which allows straightforward *igraph* representations of stream networks and easy modification of non-perennial stream DAG topologies based on water presence/absence data. The *streamDAG* package includes a wide variety of local and global measures for both unweighted and weighted stream digraphs, and provides procedures for generating Bayesian posterior distributions of the probability and the reciprocal probability of surface water presence. We demonstrate *streamDAG* algorithms using two North American non-perennial streams: Murphy Creek, a simple drainage system in the Owyhee Mountains of southwestern Idaho, and Konza Prairie, a relatively complex stream network in central Kansas.

Keywords

Non-perennial stream, Graph theory, Directed acyclic graph, Hydrologic connectivity, **R** computational software

Software / Data Availability

Software name: *streamDAG*

Developer: Ken Aho

Contact information: ahoken@isu.edu

Year first available: 2022

Hardware required: **R**-amenable frameworks, e.g., PC, tablet, laptop

System Software: Windows, Linux/Unix, MacOS

Required application software: **R** https://www.r-project.org/ (open source)

Program language: **R**

Program size: 54 kb

Repository: https://github.com/moondog1969/streamDAG (open source)

1. Introduction

By definition, non-perennial stream networks will vary in their spatial extent, complexity, and hydrologic connectedness over time. Thus, metrics for these non-perennial stream characteristics must be amenable to spatiotemporal dynamics while providing consistent summaries of networks and network components. These efforts, however, are challenged by the lack of a broad consensus concerning the meaning of important descriptive terms, including hydrological connectivity (Freeman et al., 2007, Ali and Roy, 2009; Bracken et al., 2013), and a general research and monitoring focus on perennial over non-perennial streams (Krabbenhoft et al., 2022). For example, a large number of existing measures of hydrological connectivity are spatially explicit but time invariant because of their reliance on topography, slope, and drainage area. Examples include lumped parameter basin models (Beven and Kirkby 1979), the field index of connectivity (Borselli et al. 2009), Hillslope-Riparian Stream connectivity (HRS; Jencso et al. 2009), the network index (Lane et al. 2009), and the Topographic Wetness Index (TWI, Sørensen et al. 2006). Other common approaches, including Integral Connectivity Scale Length (ICSL; Western et al. 2001) and its variants (e.g., subsurface and outlet ICSL; Ali and Roy 2010) and autocorrelation-based summaries (Knudby and Carrerra 2005, Ali and Roy 2010), allow tracking of stream network connectivity over time, but do not quantify the relative importance of particular stream locations to whole-network functionality.

An alternative approach considers stream topology from the perspective of graph theory. This method appears particularly useful for representing non-perennial streams because it provides straightforward standard graphical and numerical tools for the tracking of a stream network as its sections dry. Importantly, graph theoretic methods allow network level summaries as well as consideration of the potential importance of individual stream locations to the functioning of the overall network. A number of recent attempts have been made to apply graph theory perspectives to stream networks. These include the use of graph betweenness centrality to identify critical stream network nodes (Sarker et al. 2019), the modelling of stream flow fluctuations using directed visibility graphs in time series analyses (Serinaldi and Kilsby 2016), conflating graph-theoretic and percolation theory perspectives to measure connectivity (Larsen et al. 2012), physics-guided graph models of stream connectivity (Jia et al. 2021), the use of nested subgraphs for measuring aquatic organism dispersal among reaches (Baldan et al. 2022), and directed graph streamflow models with neural networks (Liu et al. 2022). Unfortunately, a lack of a rigorous but accessible framing of stream systems in the context of graph theory has prevented even more widespread applications of this unifying approach. In this paper, we address this deficiency by: 1) demonstrating representations of non-perennial stream networks as directed acyclic graphs, 2) reviewing and identifying graph-theoretic approaches of greatest practical usefulness for the analysis of these networks, and 3) developing and applying computational algorithms for these graph-theoretic approaches, contained in a new **R** software package: *streamDAG*. We use *streamDAG* functions to describe and compare two non-perennial streams with putatively distinct network characteristics.

1.1 Non-perennial streams as DAGs

In general, a directed graph (digraph) is an ordered pair $D = (N, A)$, where N is a set of *nodes* and A is a set of *arcs* that link the nodes. The *order* of a digraph, also called the *nodal cardinality*, is the number of digraph nodes, and is denoted as $n = |N|$, whereas the *size* of a digraph is the number of arcs. The size of a digraph is also called the *arc cardinality*, and is denoted $m = |A|$. If $z \in A$ is an arc from node u to node v, we denote this as $z = \overrightarrow{uv}$. This specification defines node u as the *tail* of arc z and v as the *head* of z. In a digraph we can distinguish the *indegree* and *outdegree* of a node as the number of arcs with that node as head and the number of arcs with that node as tail. The *degree* of a node is the sum of its indegree and outdegree.

Streams networks can be represented using graphs, with streams segments as arcs bounded by nodes occurring at hydrologically meaningful locations such as sensor sites, network confluences or splits, sources, sinks (Dodds and Rothman 2000, Rinaldo et al. 2006). Because they are strongly driven by hydrological potentials resulting from fixed elevational gradients, graphs that are most appropriate for describing passive stream network characteristics such as transport and discharge, will be both directed (with an orientation from sources to sink) and acyclic (Fig 1). A graph *cycle* occurs when a *path* starts and ends at the same node.

The directed acyclic graph (DAG) in Fig 1a represents a hypothetical stream with 14 arcs (stream segments) and 15 nodes (stream point locations separating segments). Specifically, $N = \{a, b, c, d, e, f, g, h, i, j, k, l, m, n, o\}$, and $A = \{\overrightarrow{ab}, \overrightarrow{be}, \overrightarrow{cd}, \overrightarrow{de}, \overrightarrow{ej}, \overrightarrow{jm}, \overrightarrow{fg}, \overrightarrow{gi}, \overrightarrow{hi}, \overrightarrow{ik}, \overrightarrow{lm}, \overrightarrow{mn}, \overrightarrow{no}\}$. In Fig 1a we note that all nodes except the sink node have outdegree one and that all nodes except those at sources and junctions have indegree one.

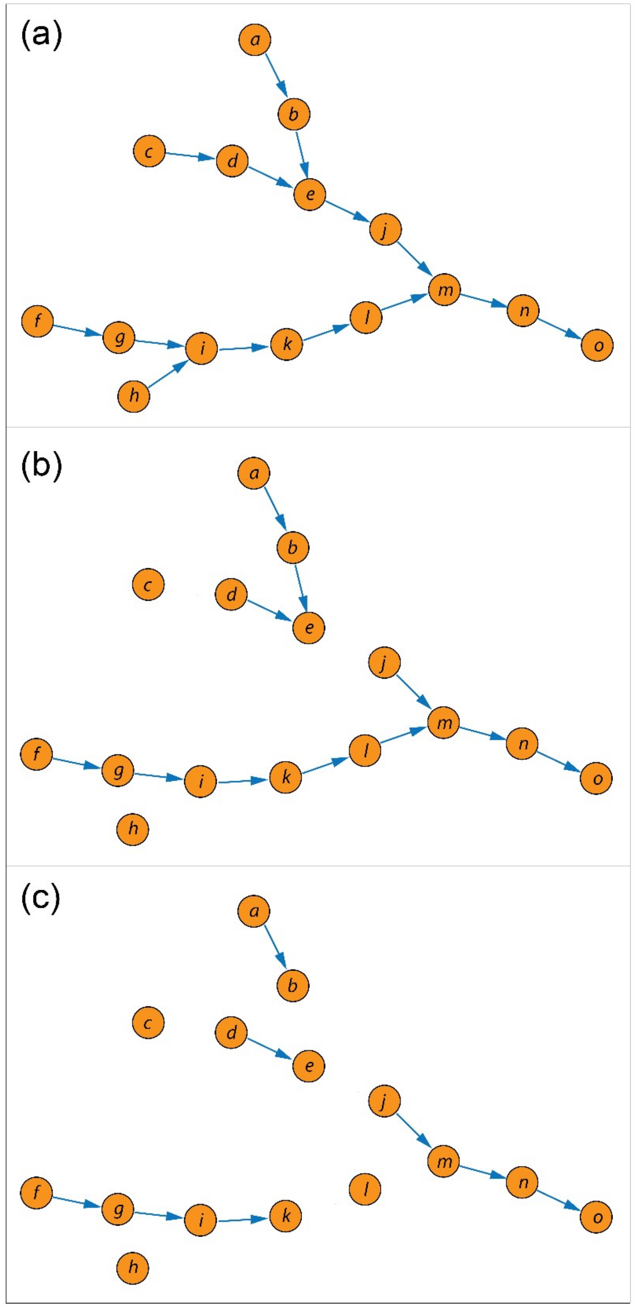

Figure 1. A series of DAGs representing a drying stream network over time. Nodes are lettered and arcs are indicated with arrows indicating flow direction. The stream dries from (a) all arcs (segments) present, to (b) three arcs absent, to (c) six arcs absent.

A digraph is *strongly connected* if every node is reachable from every other node. A digraph is *weakly connected* if every node is reachable after replacing all oriented arcs with bidirectional arcs. In a *disconnected* digraph, there will exist at least two nodes that cannot be connected, even with bidirectional arcs. Since water flows in only one direction in stream networks (uphill to downhill), there are no bidirectional arcs, and streams DAGs are never strongly connected. As non-perennial stream networks dry, stream DAGs transition from weakly connected (Fig 1a), to disconnected (Fig 1b,c).

Graphs can be represented with an $n \times n$ *adjacency matrix*, $\mathbf{A}$, whose entries, A_{ij}, indicate that an arc exists from node i to j, with $A_{ij} = 1$, or that there is no arc from i to j, with $A_{ij} = 0$. The adjacency matrix can be used to describe many network characteristics. For instance, by applying the definition of matrix multiplication, the i, j entry in $\mathbf{A}^k$ will give the number of paths in the graph from node i to node j of length k. For example, computation of $\mathbf{A}^6$ for the adjacency matrix from the stream network in Fig 1a reveals five paths of length six. These paths start at nodes a, c, f, g, h, and all but one ends at the sink node, o. The paths are: (a, b, e, j, m, n, o), (c, d, e, j, m, n, o), (f, g, i, k, l, m, n), (g, i, k, l, m, n, o), and (h, i, k, l, m, n, o). Other, more complex, matrix representations of graphs include the distance matrix, and the graph Laplacian and its variants (see Newman 2018).

We note that our treatment of digraphs here is intentionally simplistic and does not include all possible approaches for describing DAGs. For instance, we do not consider the vast array of methods associated with the detection of network community structures (e.g., *spectral cluster analysis*; Newman 2006). Thorough mathematical considerations of digraphs and graphical networks are given in Bang-Jensen and Gutin (2007) and Newman (2018), respectively.

2. Purely topological measures for describing non-perennial streams

Graph-theoretic approaches for describing stream DAGs can be separated into *local measures* that describe the characteristics of individual nodes or arcs (Table 1), and *global measures* that summarize the characteristics of an entire digraph (Tables 2-4). See Appendix A (Table S1) for measures that may not be useful for stream digraphs.

2.1 Local measures

2.1.1 Centrality. A common measure of nodal importance is the *centrality* of a node. Many metrics of centrality have been proposed, reflecting myriad perspectives on graph centrality (Bonacich 1987). These include degree centrality (i.e., the nodal degree), eigenvector centrality (Bonacich 1972, 1987), authority centrality (Kleinberg 1999), closeness centrality, betweenness centrality, information centrality (Brandes and Fleischer, 2005), and random walk betweenness (Newman 2005), among others (Borgatti 2005). See Borgatti and Everett (2006) for a mathematical classification of centrality indices, and Schoch and Brandis (2016) for a unifying perspective on these measures.

Unfortunately, many centrality approaches will be uninformative, incalculable, or analytically problematic for DAGs. For example, in a stream DAG all nodes aside from sources, sinks, confluences, and splits will have the same indegree and outdegree and hence the same *degree centrality*. *Eigenvector centrality*, the corresponding entry in the principal eigenvector of the graph adjacency matrix, extends degree centrality by accounting for a node's connection to nodes that are themselves important (Newman 2018). However, because the adjacency matrix of a directed graph will be asymmetric, it will have distinct left- and right-hand eigenvectors. In analyses of stream DAGs, one might use the right-hand principal eigenvector because centrality measures of a node will then be based on upstream input nodes (Newman 2018). However, other problems arise including the fact that source nodes, which must have indegree zero, will drive all downstream nodes to have an eigenvector centrality of zero (Newman 2018, pg. 162).

One solution to this problem is *alpha* or *Katz centrality* (Katz 1953, Bonacich and Lloyd 2001) which, following Newman (2018), is defined for all nodes simultaneously by

$$\boldsymbol{x} = (\boldsymbol{I} - \alpha \boldsymbol{A})^{-1}\boldsymbol{1}, \tag{1}$$

where $\boldsymbol{I}$ is the $n \times n$ identity matrix, $\boldsymbol{1} = (1,1,\ldots,1)$ with n entries, and α is a user-defined constant that allows weighting all nodes with a small but nonzero amount of initial centrality. Many researchers define α to be slightly less than the reciprocal of the primary eigenvalue because such a number: 1) allows the computational convergence of Eq 1, and 2) results in an outcome similar to eigenvector centrality. The alpha centrality algorithm from the network analysis package *igraph* (Csardi and Nepusz 2006) uses α = 1 by default. The *PageRank* metric (Brin and Page 1998), is similar to alpha centrality, but ensures that the centrality of a node is proportional to the centrality of the neighbors of the node divided by their outdegree (Newman 2018). Newman (2018, pg. 165) explains a method for addressing terms with outdegree zero.

Originally developed to describe interactions of social groups, *closeness centrality* (Bavelas 1950) measures the mean shortest path distance from a node to all other nodes. This metric is also poorly suited to stream networks because a DAG will not be strongly connected (Fig 1), and thus some conceptual internodal distances must be infinite. To account for this, *improved closeness centrality* (Beauchamp, 1965) is based on the reciprocals of nodal shortest path distances from the ith node to all other nodes, $1/\delta_{i,j}$ where $j \neq i = 1,2,\ldots,n-1$, allowing application to weakly connected or disconnected digraphs. The *improved closeness centrality* for the ith node is:

$$C_i = (n-1)\sum_{i \neq j} \frac{1}{\delta_{i,j}} \tag{2}$$

where, for disconnected nodes, the reciprocal distance $1/\infty$ is taken to be zero. Improved closeness centrality has been described in the literature under several names, including *harmonic centrality* (Rochat 2009) and *valued centrality* (Dekker 2005).

Nodal betweenness centrality (Freeman 1977) measures the extent to which a node lies along network paths. The nodal betweenness centrality of the *i*th node has the form:

$$B_i = \sum_{uv} \frac{n_{uv}^i}{g_{uv}} \tag{3}$$

where n_{uv}^i is the number of shortest paths from node *u* to node *v* that pass-through node *i*, and g_{uv} is the total number of shortest paths from *u* to *v*, which is at most one if there are no splits. In the case that g_{uv} = 0 (and hence $n_{uv}^i = 0$) the ratio is assumed to be 0. Thus, unlike other centrality measures, nodal betweenness centrality is not necessarily a measure of how well-connected a node is, but a measure of how often a node falls between other nodes. In stream DAGs, nodal betweenness centrality will be highest at confluences or splits, and at locations near the middle of reaches, and lowest near source and sink nodes. Betweenness of arcs can also be calculated. Specifically, *arc betweenness* is the number of shortest paths that pass through an arc (Girvan and Newman 2002).

2.1.2 Summaries of paths and distances. The connectivity and importance of a stream node can be considered by summarizing the distribution of its path lengths using conventional descriptive statistics. Path lengths include the lengths of paths that *end at* a particular node (*in-path lengths*) and path lengths that *begin* at a particular node (*out-path lengths*). Thus, no in-paths will exist for source nodes and no out-paths will exist for sink nodes. In the summarization of stream DAGs, in-paths are likely to be of greater interest than out-paths because the former considers the capacity of a node to be an intermediate or final repository of upstream information (Newman 2018, pg. 162). The most common statistical summary of nodal path lengths is *mean path length* (Albert and Barabási 2002). However, node-level topological nuances may be revealed by other statistical measures, such as the heterogeneity of path lengths (e.g., the sample variance) and the symmetry and peakedness of path length distributions (e.g., the sample skew and kurtosis) of a node.

For stream DAGs it is often reasonable to ignore nonexistent upstream and disconnected paths (see discussion in Newman 2018, pg. 133). This allows computation of the *eccentricity* of a DAG node, i.e., the longest path distance between a node and all other nodes. The maximum DAG in-path length to the ith node is the *in-eccentricity* of the ith node (often called *height*). The maximum DAG out-path length from the ith node is the *out-eccentricity* of the ith node. The reciprocal of the distance between nodes i and j defines their *efficiency* (Latora and Marchiori 2001). Reflecting the constraints of improved closeness centrality, efficiencies based on infinite (upstream or disconnected) distances are generally taken to be zero. In DAGs, *in-efficiencies* (based on in-paths) will be distinct from *out-efficiencies* (based on out-paths), allowing calculations of average in-and out-efficiency for individual nodes to quantify local connectedness. Note that the overall mean efficiency of the ith node (based on both in-efficiencies and out-efficiencies) will be the improved closeness centrality of the ith node (Eq 2), times $\frac{1}{n(n-1)}$.

2.1.3 Visibility. Visibility graphs (Lacasa et al. 2008, Luque et al. 2009, Lacasa and Toral 2010) allow summaries of nodal importance based on the *visibility* of nodes to other nodes within a sequential series. Specifically, nodes i and j will be visible to each other if, when node data are plotted as vertical bars (with bar heights designating nodal data outcomes), and bars are placed along the abscissa based on some ordering of nodes in the stream network, the tops of bars for nodes i and j can be connected with a straight line, uninterrupted by other bars (see Lacasa et al. 2008, Luque et al. 2009). See Section 4.5 for a description of nodal ordering approaches used by the software package *streamDAG* in the context of visibility.

In a stream DAG, a node will always be visible from the node directly upstream (and vice versa), regardless of data outcomes, and nodes with larger data outcomes will be able to “see” more nodes and be “more visible” to other nodes than those with smaller outcomes. One potential source of nodal data for visibility graphs is the indegree or outdegree of the nodes themselves. Under this approach, high degree locations, located at stream junctions or splits, may block visibility of downstream nodes from upstream nodes, and vice versa.

2.1.4 Stream order. Several topological measures of branching complexity specific to stream networks have been proposed under the name *stream order*, not to be confused with *graph order* (the number of graph nodes). *Strahler stream order* (Strahler 1957) is a "top down" system in which first order stream sections (and their associated nodes and arcs) occur at the outermost tributaries. A stream section resulting from the merging of tributaries of the same order will have a Strahler order one unit greater than the order of the tributaries. That is, a stream section downstream of a confluence of two first-order tributaries will be second-order. A stream section resulting from the merging of tributaries of different order will have the Strahler stream order of the tributary with the larger Strahler number. Under *Shreve stream order* (Shreve 1966), a stream section resulting from the merging of tributaries will always have an order that is the sum of the order of those tributaries.

Some considerations are necessary for nodal stream order in disconnected stream DAGs. One approach is to calculate stream order only for nodes in the subgraph containing the sink. This is the method used by the software package *streamDAG*. As an alternative, one could define separate subgraphs for each disconnected portion of the network and calculate nodal stream order within the context of each subgraph.

Metric	Definition and details	Type of summary
Number of nodes reachable from the *i*th node	Section 1.1	Nodal connectivity. Will emphasize source nodes.
Number of paths that reach *i*th node	Section 1.1	Nodal connectivity. Will emphasize sink nodes
Length of the upstream network ending at (draining into) the *i*th node	Section 1.1	Nodal centrality
Alpha centrality of *i*th node (Katz 1953, Bonacich and Lloyd 2001)	See Eq 1, and details in Newman (2018)	Nodal centrality
PageRank centrality of *i*th node (Brin and Page 1998)	See details in Newman (2018)	Nodal centrality
Improved closeness centrality of *i*th node (Beauchamp 1965)	See Eq. 2	Nodal centrality
Nodal betweenness centrality of *i*th node (Freeman 1977)	See Eq. 3	Nodal betweenness
Arc betweenness of the *k*th arc (Girvan and Newman 2002)	The number of shortest paths that pass through the *k*th arc	Arc betweenness
Visibility of the *i*th node to and from other nodes	See Luque et al. (2009)	Nodal importance
Strahler stream order (Strahler 1957) or Shreve stream order (Shreve 1966) of the *i*th node or *k*th arc.	See description in the Stream Order section	Node or arc nestedness
Statistical summaries of upstream in-path lengths to the *i*th node and downstream out-path lengths from the *i*th node; e.g., mean, median, max, min, variance, skew, kurtosis. Stream path maxima constitute measures of eccentricity.	See Aho (2014).	Nodal centrality and topological nuance
Average in- and out-efficiency of the *i*th node (Latora and Marchiori 2001) or both together.	Average of reciprocal distances	Nodal connectivity
Statistical summaries of degrees of nodes in upstream in-path lengths and downstream out-path lengths for the *i*th node; e.g., mean, median, max, min, variance, skew, kurtosis	See Aho (2014)	Nodal complexity, connectivity, and/or topological nuance

Table 1. Local (generally nodal) unweighted graph metrics appropriate for stream DAGs.

2.2 Global measures

Global DAG measures allow consideration of a stream network in its entirety. Statistical summaries (e.g., mean, median, variance) of local metrics, including degree and path lengths provide one global approach. For instance, the mean of all path lengths in a graph is a frequently used global metric. Other global path length summaries include *graph diameter* (the maximum eccentricity across all nodes) and the *graph radius* (the minimum eccentricity across all nodes). While rarely applied for this purpose, contraction and expansion of a non-perennial stream network will produce changes in the global stream order which can be used to track changes in a stream's network structure by considering network components with active surface flow rather than the geomorphic channel network (Godsey and Kircher 2014). The global Strahler stream or global Shreve stream order is the stream order of the sink node, which will be the maximum nodal stream order of the network (or sink sub-network in disconnected stream DAGs).

2.2.1 Global efficiency. Global metrics that calculate sums of path distances, including the *Wiener index* (Wiener 1947) and the *hyper-Wiener index* (Randić 1993), are problematic for non-perennial stream DAGs, because as noted above, distances between disconnected nodes (and distances from downstream to upstream nodes) will be infinitely large. Several metrics, including *global efficiency* (Ek et al. 2015), *the Harary index* (Plavšić et al. 1993), and *Balaban's J-index* (Balaban 1982), address this problem by considering scaled sums of nodal reciprocal distances, i.e., the nodal efficiencies.

The global efficiency of a digraph D is simply the mean of all pairwise nodal efficiencies:

$$E(D) = \frac{1}{n(n-1)} \sum_{1 \le i < j \le n} e_{i,j}, \tag{4}$$

where the efficiency between nodes i and j, for all $i \neq j$, is defined as $e_{i,j} = 1/\delta_{i,j}$, where $\delta_{i,j}$ is the distance from node i to node j in D. Global efficiency is closely related to the Harary index:

$$H(D) = \frac{1}{2} \sum_{1 \le i < j \le n} e_{i,j} = \frac{n(n-1)}{2} E(D). \tag{5}$$

2.2.2 I(D) metrics. A large number of global DAG metrics relevant to non-perennial streams share the same formulaic basis. Specifically, for an arc $a = \overrightarrow{uv}, a \in A$, denote the outdegree of u as d_u^+, and the indegree of v as d_v^-. Now, let $I(D)$ represent a general topopological index for a digraph, D, that depends on d_u^+ and d_v^-:

$$I(D) = \frac{1}{2} \sum_{uv \in A} \omega\,(d_u^+, d_v^-). \tag{6}$$

Four basic configurations can be recognized (Deng et al. 2022):

1. If $\omega(x, y) = (xy)^\alpha$, then $I(D)$ is the directed *Randić index* for *D* if $\alpha = -\frac{1}{2}$ (Randić 1975), the *second Zagreb index* if $\alpha = 1$ (Gutman 1975), and the *second modified Zagreb index* if $\alpha = -1$ (Anthony and Marr, 2021).

2. If $\omega(x, y) = (x + y)^\alpha$, then $I(D)$ is the directed *sum-connectivity index* for *D* if $\alpha = -\frac{1}{2}$ (Zhou and Trinajstić, 2009, Zhong 2012), and the directed *first Zagreb index* if $\alpha = 1$ (Gutman 1975). Further, if $\omega(x, y) = 2(x + y)^{-1}$, then $I(D)$ is the directed *harmonic index* of *D* (Favaron et al., 1993).

3. If $\omega(x, y) = \sqrt{\frac{x+y-2}{xy}}$, then $I(D)$ is the directed *atom bond connectivity* of *D* (Estrada et al., 1998).

4. If $\omega(x, y) = \frac{\sqrt{xy}}{\frac{1}{2}(x+y)}$, then $I(D)$ is the directed *geometric-arithmetic index* for *D* (Vukičević and Furtula 2009).

Kincaid (1996) defined a generalized Randić index for digraphs that allowed variation in indegree and outdegree designations for arc head and tail nodes. Specifically, for an arc $\overrightarrow{uv} \in A$, let $\gamma, \tau \in \{-, +\}$ index the degree type: $- = in$, $+ = out$. Then four combinations of d_u^γ, d_v^τ exist: d_u^+, d_v^-, d_u^-, d_v^-, d_u^+, d_v^+ and d_u^-, d_v^+, resulting in four different versions of any *I*(*D*) metric.

The d_u^+, d_v^- basis used in Eq. 6 is the most commonly applied (e.g., Anthony and Marr 2021, Monsalve and Rada 2021a,b, Deng et al. 2022, Arizmendi and Arizmendi 2022), and we recommend its use in the analysis of stream networks for three reasons. First, the Randić index, the second modified Zagreb index, and atom bond connectivity will contain undefined terms for arcs that include source or sink nodes, for variants of Eq. 6 that incorporate d_u^- or d_v^+, respectively. Conversely, the recommended d_u^+, d_v^- basis will be defined for any DAG arc, including those in disconnected graphs. Second, *I*(*D*) metrics using the d_u^+, d_v^+ basis will ignore the presence of joins (confluences), and variation in the number of arcs at particular joins, and similarly *I*(*D*) metrics using the d_u^-, d_v^- basis will ignore the presence of splits (e.g., islands), and variation in the number of arcs at particular splits. The d_u^+, d_v^- basis, on the other hand, allows consideration of the presence and character of both joins and splits. Finally, the recommended d_u^+, d_v^- basis is more compatible with the directed line graph of a stream DAG. The directed line graph of $D = (N, A)$ has nodes that correspond to the arcs of *D* and, for $\overrightarrow{uv}, \overrightarrow{wz} \in A$ there will be a directed line graph arc from $\overrightarrow{uv}$ to $\overrightarrow{wz}$ when $v = w$ (Harary and Norman 1960). With the d_u^+, d_v^- basis, atom bond connectivity involves the ratio of the degree of an arc, or a node in the line graph, to the product of the node degrees in the original digraph (Estrada et al. 1997).

Figure 2 shows *I*(*D*) metrics for stream-like DAGs of presumed increasing complexity under the recommended d_u^+, d_v^- basis. For these examples, all $I(D)$ indices are monotonically nondecreasing with increasing graph order when other DAG components (e.g., joins, splits, number of arcs at particular joins or splits) are held constant. For instance, every metric except atom bond connectivity (which stays constant) increases from graph 1 to 2, and from graph 3 to 4 (Fig 2A, B). For both of these graph pairs, graph order is increased by adding a node to the longest path, while other graph components remain unchanged. In general, *I*(*D*) metrics with $\omega(x, y) = (xy)^\alpha$ will equal $\frac{n-1}{2}$ for an unbranched path on *n* nodes, and will equal $\frac{n-k-1+k^{\alpha+1}}{2}$ for a digraph of graph order *n*, with *k* arcs occurring at a single join or split. Therefore, for these digraphs, the directed Randić index (for which $\alpha = -1/2$), decreases with increased branching complexity, given fixed graph order (see graphs 4-6 in Fig 2). The same trend is empirically evident for the directed modified second Zagreb index, the directed harmonic index, the directed geometric-arithmetic index, and directed sum-connectivity (Fig 2B). This trend is reversed, however, for directed atom bond connectivity and the directed first Zagreb index (Fig 2B). Clearly, the directed atom bond connectivity numerator, $\sqrt{x + y - 2}$, will equal zero when arcs are part of an unbranched path, causing the index summation to remain unchanged unless a join or split occurs. The simple additive form of the directed first Zagreb index, $\omega(x, y) = x + y$, will cause the metric to increase with both increasing path lengths and increasing branch complexity (Fig 2B).

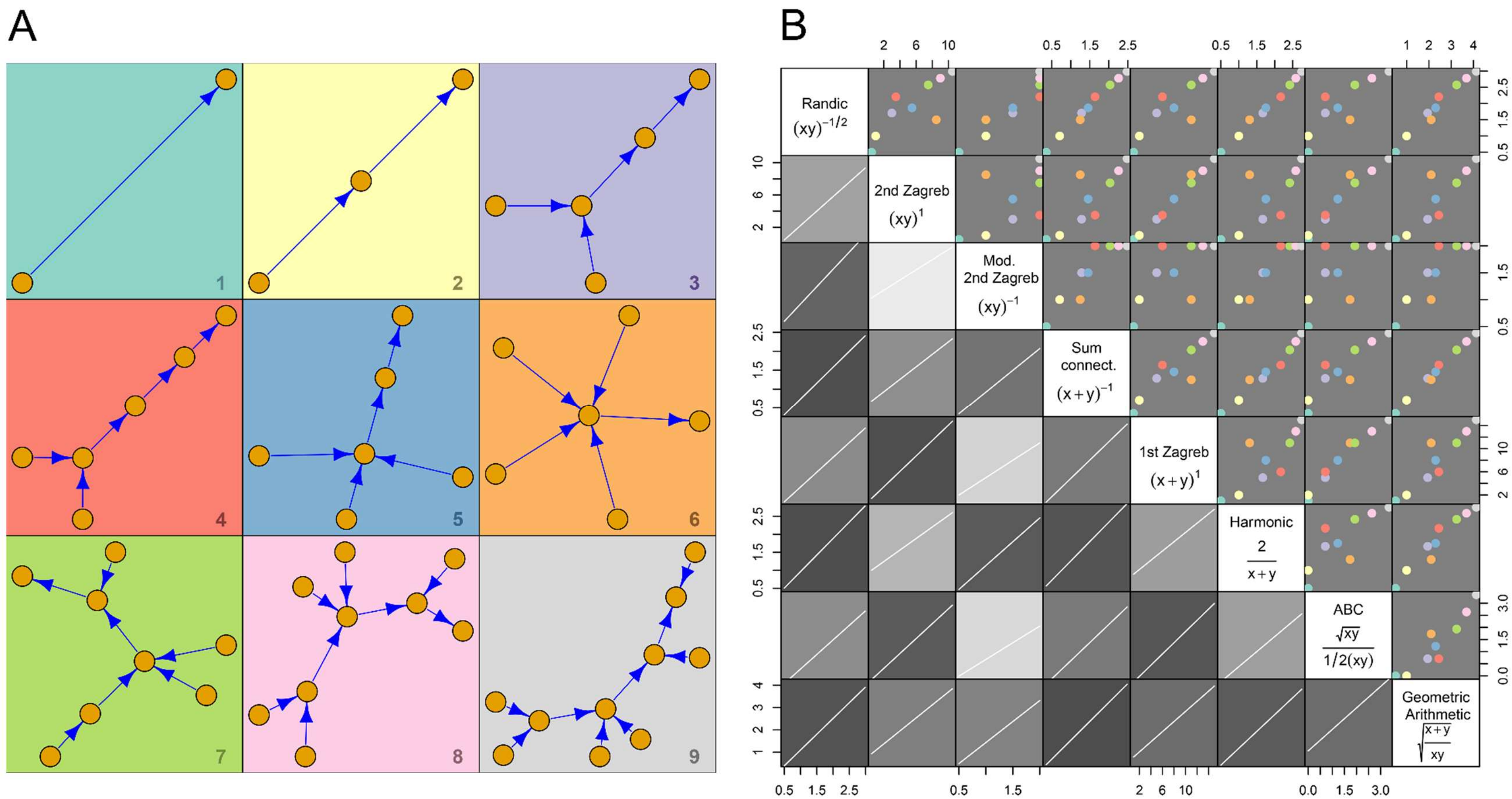

Figure 2. $I(D)$ metrics for nine DAGs of increasing complexity. Fig A shows DAGs under consideration. Fig B compares metric assessments of DAGs from A using corresponding point colors (used as backgrounds in A) in the upper triangle of B. Fits in B (shown in the lower triangle) are from simple linear regressions. Darker backgrounds in the lower triangle of B denote stronger correlations. Metrics follow a d_u^+, d_v^- basis. Although graphs in A were user-defined to encompass a range of potential network topologies, methods for the generation of random DAGs are described in Karrer and Newman (2009).

Multiplicative forms of Eq 5 have also been proposed,

$$I_m(D) = \frac{1}{2}\prod_{uv \in A} \omega\,(d_u^+, d_v^-),$$

resulting in multiplicative versions of the directed Zagreb indices (Bozovic et al., 2016; Eliasi and Ghalavand, 2016), directed sum connectivity (Bhanumathi and Rani, 2018), the directed Randić index (Gutman et al., 2018) and the directed harmonic index (Bhanumathi and Rani, 2018). Given their novelty, however, these indices are not considered further here.

2.2.3 Assortativity. Several *I*(*D*) metrics, including the normalized Randić index, may provide information concerning graph assortativity (Kincaid *et al.*, 2016), that is, the preference of network nodes to attach to others with similar degree. However, the definitive measure of graph assortativity is the *assortativity coefficient*, which is Pearson's correlation of the degree of pairs of adjacent nodes (Newman, 2002). Let $\overrightarrow{u_i v_i} \in A$ define nodes and directionality of the *i*th arc, $i = 1,2,3,\ldots,m$. Now, let $\gamma, \tau \in \{-,+\}$ index the degree type: $- = in$, $+ = out$, and let (u_i^γ, v_i^τ), represent the γ- and τ-degree of the *i*th arc. Then, the general form of the assortativity coefficient is:

$$r(\gamma,\tau) = m^{-1}\frac{\sum_{i=1}^{m}\left(u_i^\gamma - \bar{u}^\gamma\right)\left(v_i^\tau - \bar{v}^\tau\right)}{s^\gamma s^\tau} \tag{7}$$

where $\bar{u}^\gamma$ and $\bar{v}^\gamma$ are the arithmetic means of the u_i^γs and v_i^τs, i.e., $\bar{u}^\gamma = m^{-1}\sum_{i=1}^{m} u_i^\gamma$, and s^γ and s^τ are the population standard deviations of the u_i^γs and v_i^τs, i.e., $s^\gamma = \sqrt{m^{-1}\sum_{i=1}^{m}\left(u_i^\gamma - \bar{u}^\gamma\right)^2}$. Reflecting considerations given for *I*(*D*) metrics earlier, there are four possible forms to $r(\gamma,\tau)$ based on the indegree and outdegree designations of arc head and tail nodes (Foster et al., 2010). These are: $r(+,-)$, $r(-,+)$, $r(-,-)$, and $r(+,+)$ (Table 4). The correlations $r(+,+)$ and $r(+,-)$ will rarely be finite for stream networks because the outdegree of u will almost always be 1, resulting in $s^\gamma = 0$. Given constraints of Pearson's correlation, $r(\gamma,\tau)$ outcomes of zero indicate no assortative mixing, whereas positive or negative values indicate assortative or disassortative mixing, respectively. In stream DAGs, the correlations $r(-,-)$ and $r(-,+)$ will generally be disassortive because of the characteristic strong convergence of stream paths from sources to sink (e.g., Fig 1 in Foster et al., 2010) in most stream networks.

Metric	Definition and details	Type of summary
Graph diameter = *Height* of the sink	The length of the longest (non-infinite) path. Equivalent to the *in-eccentricity* of the sink.	Complexity
Graph order	No. of nodes = n	Complexity
Size	No. of arcs = m. The maximum size of a digraph is $n(n-1)$	Complexity
Number of source nodes and/or distinct stream reaches	See examples in Figs. 1 and 2	Complexity
Number of paths to sink	See examples in Figs. 1 and 2	Complexity and or connectivity
Global Strahler number (Strahler 1957) or global Shreve stream number (Shreve 1966)	Strahler or Shreve stream order of the sink node	Complexity and nestedness
Distributional estimates of upstream in-path lengths for the sink node, or entire network, and/or downstream out-path lengths for the entire network; e.g., mean, median, max, min, variance, skew, kurtosis	For descriptions of statistical estimators, see Aho (2014).	Complexity, connectivity and/or topological nuance
Statistical summaries of the global degree distribution e.g., mean, median, max, min, variance, skew, kurtosis.	For descriptions of statistical estimators, see Aho (2014). Scientific insights can also be gained by considering the viability of theoretical degree distributions of graphs, including random (Erdős and Rényi 1959), chaotic (Lacasa and Toral 2010), or scale-free (Li et al. 2005).	Complexity and/or topological nuance
Global efficiency (Ek et al. 2015)	See Eq. 4	Connectivity
Harary index (Plavšić et al. 1993)	See Eq. 5	Connectivity

Table 2. Simple unweighted global metrics appropriate for stream DAGs.

Metric	$\omega(x, y)$	Type of summary
Randić index (Randić 1975), second Zagreb index (Gutman 1975), second modified Zagreb index (Anthony and Marr, 2021).	$(xy)^{\alpha}$	Complexity, assortativity, and/or connectivity
Sum connectivity (Zhong 2012) first Zagreb index (Gutman 1975)	$(x + y)^{\alpha}$	Complexity and/or connectivity
Harmonic index (Favaron et al., 1993)	$2(x + y)^{-1}$	Complexity, connectivity and/or assortativity
Atom-bond connectivity (Estrada et al., 1998)	$\sqrt{\frac{x + y - 2}{xy}}$	Network stability and (in the context of chemical graphs) strain energy (Das et al., 2011); will increase with branching complexity.
Geometric-arithmetic index (Vukičević and Furtula, 2009)	$\frac{\sqrt{xy}}{\frac{1}{2}(x + y)}$	Complexity and/or connectivity

Table 3. Global metrics for stream DAGs from the $I(D)$ basis given in Eq. 6.

Metric	Definition	Type of summary	Extremal value
Assortativity index (Newman, 2002)	$r(\gamma, \tau)$	Assortativity	min = -1, max = 1

Table 4. Global assortativity metrics for stream DAGs from the $r(\gamma, \tau)$ basis given in Eq. 7.

3. Weighted graphs

While purely topological measures may be useful in describing local importance and global connectivity in stream DAGs, they will be strongly affected by user-defined node designations and abstracted from many important characteristics of stream networks. Realism can be enhanced in stream DAGs by adding information to nodes and/or arcs in the form of *weights*. Weighting information particularly relevant to non-perennial stream DAGs include flow rates, stream lengths, probabilities of aquatic organism dispersal, inputs of water quality constituents such as nutrients or sediment (i.e., *loading*; Maidment 1996), upstream drainage area, and/or probabilities of surface and subsurface water presence. Notably, a number of weighted measures described here were developed outside the explicit realm of graph-theory. They are included because of their prior use in describing stream networks and their straightforward extendibility to a weighted digraph framework.

Graph weights can be extremely simple and flexible. Consider degree centrality, which, as noted earlier, will be largely invariant for stream DAGs. By adding weights to arcs, weighted degree centrality variants may contain much more information and realism. For instance, in Fig 1a, the nodes *e* and *i* both have indegree = 2 and outdegree = 1. However, assume that the arcs $\overrightarrow{be}, \overrightarrow{de}, \overrightarrow{ej}$ and $\overrightarrow{gi}, \overrightarrow{hi}, \overrightarrow{ik}$ have the stream lengths 20m, 30m, 40m, 50m, 60m, 70m, respectively, and that we wish to use those lengths as weights. We could sum the weights of bounding arcs to obtain a nodal measure called *strength centrality* (Barrat et al. 2004). Now node *e* has indegree 50, and outdegree 40, and node *i* has indegree 110, and outdegree 70, emphasizing the potential network importance of node *i* over node *e*. As with non-weighted stream DAGs, both local and global summaries are possible for weighted stream DAGs.

3.1 Local measures

Weighted local graph metrics include strength centrality, and other weighted variants of degree centrality (e.g., Opsahl et al. 2010), weighted alpha-centrality, weighted path length summaries, and weighted *nodal diversity* (the Shannon entropy of associated arc weights) (Table 5). Two important weighted graph measures whose development was driven by non-perennial stream research are *mean Bernoulli stream length* [i.e., arc length multiplied by the probability of arc presence; Botter and Durighetto (2020)] and *mean communication distance* (i.e., arc length multiplied by the inverse probability of arc presence; Aho et al. 2023). Arcs with large communication distances will have higher propensities to become stream bottlenecks. Arc probabilities associated with Bernoulli length and communication distance can be estimated using stream presence data from nodes bounding respective arcs (Aho et al. 2023).

Under an entirely different framing of stream graphs, we can define each stream reach as an individual node and define an edge (undirected arc) between these nodes as a confluence or barrier or split between the reaches (Baldan et al. 2022). Then it is possible to let $p_{i,j}$ be the probability of organism dispersal or stream transport of materials from reach *i* to reach *j*, let w_j represent a connectivity-related weighting value for the *j*th reach, and let *W* be the sum of those weights over all *l* reaches. Then the *Reach Connectivity Index* for the *i*th reach (*RCI*; Baldan et al. 2022) can be defined as:

$$RCI_i = \sum_{j=1, j \neq i}^{l} p_{i,j} \frac{w_j}{W} \tag{8}$$

As Baldan et al. (2022, Eq. 2.5) point out, an undirected edge ij can be replaced by two oppositely directed (upstream and downstream) arcs to which $p_{i,j}$ and $p_{j,i}$ can be assigned as potentially distinct probabilities. A large number of weighting approaches are possible for Eq. 8 that are considered briefly in the next section and are considered thoroughly by Baldan et al. (2022).

Metric	Definition and details	Weights	Type of summary
Strength centrality	Sum of weights from adjoining arcs	Any arc weights	Nodal importance
Weighted alpha centrality	See description of unweighted alpha-centrality	Any arc weights	Nodal importance
Length of the upstream network ending at (draining into) the *i*th node, in measured units, e.g., meters.	Sum of weights of path arcs for a subgraph rooted at the *i*th node	Arc lengths	Nodal importance, connectivity
Statistical summaries of weighted upstream in-path lengths or downstream out-path lengths for the *i*th node; e.g., mean, median, max, min, variance, skew, kurtosis	See Aho (2014)	If actual instream arc lengths are used, provides summaries of path lengths for nodes with respect to field-measured units	Nodal importance, nodal nuance
Nodal diversity	Conventionally, Shannon entropy (Shannon 1948) of nodal arcs weights. Usually based on undirected graphs.	Any arc weights	Nodal heterogeneity and complexity,
Node weighted visibility	See description of unweighted visibility	Any node weights	Nodal importance
Average Bernoulli arc length (Botter and Durighetto 2020)	The probability of the presence of an arc times its length. Developed to describe non-perennial stream dynamics.	Arc probability (of stream activity) and arc length	Non-perennial arc nuance
Average arc communication distance (Aho et al 2023)	The inverse probability of the presence of an arc times it length. Developed to describe non-perennial stream dynamics.	Arc inverse probability (of stream activity) and arc length	Non-perennial arc nuance
Reach Connectivity Index (RCI; Baldan et al. 2022)	Developed to measure organismal dispersal (Eq. 8). Thus, generally uses an undirected graph framework.	Conventional reach weights include: length, volume, stream order and habitat area	Reach (sub-graph) connectivity

Table 5. Weighted local (nodal, arc, and subgraph) metrics.

3.2 Global measures

Several existing network-level connectivity metrics from the hydrological literature can be viewed as weighted digraph measures. These include *Integral Connectivity Scale Length* (*ICSL*): the average distance between wet nodes in a stream network (Western et al. 2001, Ali and Roy 2010), average Bernoulli stream network length: the sum of average Bernoulli arc lengths, and average network-level communication distance: the sum of average arc communication distances

(Table 6). At a particular point in time, Bernoulli stream network length is identical to instantaneous *active stream length* (cf. Durighetto and Botter 2022).

Reverting to a reach-as-node perspective, the Reach Connectivity Index (Eq. 8) can be extended to a weighted global metric, the *Catchment Connectivity Index* (*CCI*; Baldan et al. 2022):

$$CCI = \sum_{i,j=1,i\neq j}^{l} p_{i,j} \frac{w_i w_j}{W^2} \tag{9}$$

Like *RCI*, *CCI* ranges from 0 to 1, where a zero indicates the absence of connectivity and a one indicates maximum stream connectivity. Many *CCI* and *RCI* variants are possible based on the types of weights used, and approaches for viewing $p_{i,j}$ (see Baldan et al. 2022). For instance, if weights are based on reach lengths, then Eq. 9 can be viewed as the *Dendritic Connectivity Index* (*DCI*; Cote et al. 2007), and if reach volume is used as a weight variable, then Eq 8 can be seen as the *Volume-based River Connectivity Index* (Grill et al. 2014).

Metric	Definition and details	Weights	Type of summary
Integral connectivity scale length (ICSL)	The average distance over which wet locations (e.g. stream graph nodes) are connected using Euclidean distances or topographically-defined hydrologic distances (Ali and Roy 2010). Includes surface ICSL (Western et al. 2001), and subsurface and outlet ICSL (Ali and Roy 2007).	Arc lengths or Euclidean distances	Network connectivity
Weighted Harary index (Plavšić et al. 1993), weighted global efficiency (Ek et al. 2015)	See Eqs. 4 and 5	Any arc weights, including arc lengths	Network connectivity
Average strength	See description for strength	Any arc weights	Network connectivity
Average alpha-centrality	See description for unweighted alpha-centrality.	Any arc weights	Network connectivity
Weighted size of sink subgraph	Arc weights are stream segment lengths. Weights of the graph or subgraph associated with the sink node are summed.	Arc lengths	Sink-focused network connectivity and complexity
Average Bernoulli network length (Botter and Durighetto 2020)	The sum of the product of the probabilities of the presence of arcs their respective lengths. Developed specifically for describing non-perennial stream dynamics.	Arc probability and length	Network connectivity
Average network-level communication distance (Aho et al 2023)	The sum of the product of the inverse probabilities of the presence of arcs their respective lengths. Developed specifically for describing non-perennial stream dynamics.	Arc probability and length	Network connectivity
Catchment Connectivity Index (Baldan et al. 2022)	Developed for measuring connectivity with respect to organismal dispersal in streams (see Eq. 9). Thus, generally uses an undirected graph framework. Variants include: the Dendritic Connectivity Index (DCI; Cote et al. 2009), the Population Connectivity Index (PCI; Angulo-Rodeles 2021), the Probability of Connectivity (PC; Pascual-Hortal and Saura 2006), and the Volume-based River Connectivity Index (Grill et al. 2014), among others.	Conventional reach weights include: lengths, volume, stream order, and habitat area	Network connectivity

Table 6. Weighted global metrics for stream DAGs.

3.3 Bayesian extensions

Bayesian extensions to Bernoulli length and communication distance are possible by viewing the probabilities of stream presence at arcs as random variables. The complete statistical framework for these approaches is described in Aho et al. (2023). Briefly, given a beta-distribution prior for the probability of the presence of water at the *k*th arc, and a binomial likelihood for observed binary stream presence outcomes over *n* trials at the *k*th arc, the conjugate posterior beta distribution for the probability of stream presence for the *k*th arc can be expressed as:

$$\theta_k|\boldsymbol{x}_k \sim BETA(\omega \cdot n \cdot \hat{p}_k + \sum \boldsymbol{x}_k, \omega \cdot n(1 - \hat{p}_k) + n - \sum \boldsymbol{x}_k) \tag{10}$$

where ω is the weight given to the prior relative to the current data, $\hat{p}_k$ is the mean of the prior beta distribution, and hence the most likely prior probability of the *k*th arc, and $\sum \boldsymbol{x}_k$ is the number of binary successes (stream surface water presence outcomes) at the *k*th arc, over *n* trials. The posterior distribution for the inverse probability of stream presence for the *k*th arc will follow an inverse beta distribution (see Aho et al. 2023) with the same parameters shown in Eq. 10. Under linear transformation, multiplying the *k*th posterior for the probability of stream presence by the *k*th stream length will provide the *k*th posterior for Bernoulli stream length, whereas multiplying the *k*th posterior for the inverse probability of stream presence by the *k*th stream length will provide the *k*th posterior for communication distance, providing both global and local estimates for the propensity of bottlenecking (Aho et al. 2023).

4. The streamDAG package

We developed the *streamDAG* software package within the **R** computational environment (R Core Team, 2021) to provide algorithms for visualization and analysis of non-perennial stream networks, including the computation of the indices and approaches described in Sections 2 and 3. The *streamDAG* package works under the expansive graph theory package *igraph* (Csardi and Nepusz, 2006), which can be implemented under **R**, Python, and Mathematica language environments (igraph 2022).

Following installation of the **R** *devtools* package, for instance, by typing: `install.packages("devtools")` at the **R** command line, the *streamDAG* package can be installed for Windows, MacOS, and Linux/Unix-alike platforms from its GitHub repository using:

```
library(devtools)

install_github("moondog1969/streamDAG")
```

And subsequently loaded, using simply:

```
library(streamDAG)
```

Installation and loading of the *streamDAG* package will result in automatic installation and loading of the **R** *igraph* package, respectively. The *streamDAG* package will be formally released to the Comprehensive **R** Archive Network (CRAN) following publication of this manuscript.

4.1 Application

As applications for the *streamDAG* package, we considered two non-perennial stream networks: Murphy Creek, and a portion of the south fork of Kings Creek in Konza Prairie (hereafter referred to as Konza Prairie for brevity). Murphy Creek is a simple network (two sources and a single outlet) within the larger Reynolds Creek experimental watershed in the Owyhee Mountains of southwestern Idaho, USA (43.256° N, 116.817° W). Measures of surface water presence at Murphy Creek were made at 25 nodes at 15-minute intervals from 6/3/2019 to 10/3/2019. Surface water presence / absence was determined using Onset HOBO Pendant/Light 64 K Datalogger UA002-64 resistivity sensors and HOBO pressure transducers (see Warix et al., 2021). Bounding nodes were added at two theorized stream source locations and the network sink to encompass the entire length of the network. This resulted in a final Murphy Creek network with 28 nodes and 27 arcs for analysis (Fig 3a). Konza Prairie is a relatively complex non-perennial stream network in the northern Flint Hills region of Kansas, USA (39.11394° N, 96.61153°W). Our depiction of the Konza Prairie network required 46 nodes and 45 arcs, with nine source nodes and three major reaches leading to the outlet node (Fig 3b).

4.2 Data outlay

Our *igraph* codification of the complete (fully wetted) Murphy Creek network had the form:

```
murphy_spring <- graph_from_literal(IN_N --+ M1984 --+ M1909, IN_S --+
M1993 --+ M1951 --+ M1909 --+ M1799 --+ M1719 --+ M1653 --+ M1572 --+
M1452, M1452 --+ M1377 --+ M1254 --+ M1166 --+ M1121 --+ M1036 --+
M918 --+ M823, M823 --+ M759 --+ M716 --+ M624 --+ M523 --+ M454 --+
M380 --+ M233 --+ M153 --+ M91 --+ OUT)
```

The code `IN_N --+ M1984` indicates that the stream flows from node IN_N to node M1984, and so on. The designation `M1984` indicates that the node has an instream distance of approximately 1984 meters from the outlet. The Konza network uses a more complex nodal naming system based on reaches. Several non-perennial stream graphs, including the complete Murphy Creek and Konza networks can be called using the *streamDAG* function `streamDAGs`.

Purely topological analyses can be conducted in *streamDAG* using only an *igraph* codified stream network. Much more flexibility is possible, however, by incorporating ancillary information including spatial coordinates and graph weighting data. As noted earlier, weights can include, but are not limited to, arc lengths, node and arc flow rates, stream loading, and stream segment surface water presence/absence information.

4.3 Spatial plots

Spatial representations of stream DAGs can be obtained from the *streamDAG* function `spatial.plot()` by applying nodal spatial coordinates to a stream DAG object. (Fig 3). Stream shapefiles, which may capture stream segment spatial nuances (instead of arc directional arrows), can also be used by `spatial.plot()` with some loss of flexibility.

```
data(mur_coords); data(kon_coords); par(mfrow = c(2,1))

spatial.plot(murphy_spring, mur_coords$long, mur_coords$lat,
mur_coords$Object.ID)

spatial.plot(streamDAGs("konza_full"), kon_coords$long,
kon_coords$lat, kon_coords$Object.ID)
```

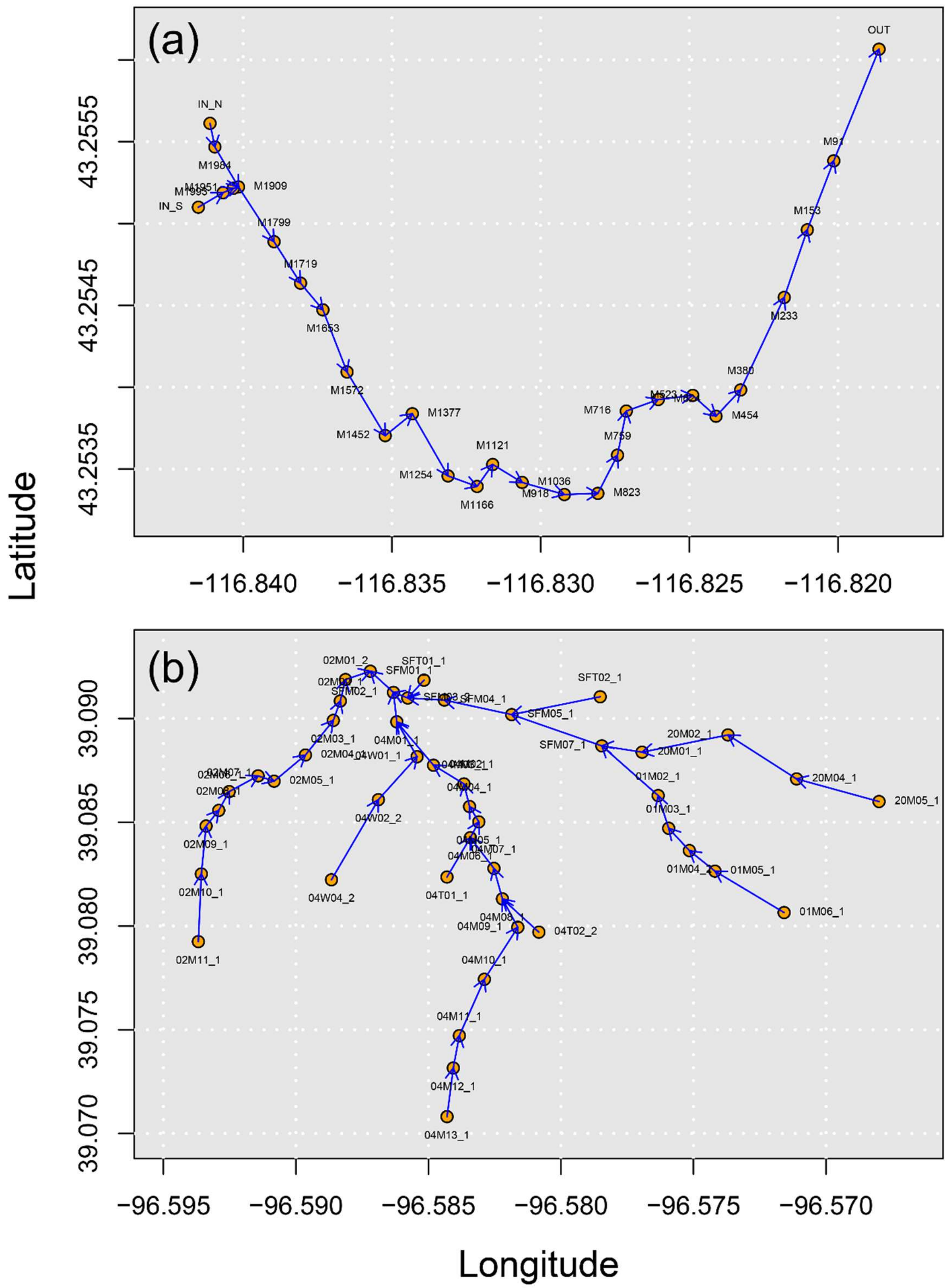

Figure 3. Spatially explicit DAG representations of (a) the completely wetted Murphy Creek network, and (b) the completely wetted Konza Prairie network. Nodes occur at stream sensor locations. Note (user-controlled) northing exaggeration in panels.

4.4 Tracking intermittency

Stream intermittency can be tracked using either node or arc presence / absence data. Below we create a new graph object, `G1`, consisting of the subset of wet nodes at timestamp 8/9/2019 22:30 (time point 650), from the dataframe `mur_node_pres_abs`. We then call `G1` to make a new Murphy Creek graph using `spatial.plot()` (Fig 4). Note that arcs missing one or more wet bounding nodes are omitted by the algorithm.

```
data(mur_node_pres_abs)
G1 <- delete.nodes.pa(murphy_spring, mur_node_pres_abs[650,][,-1])
```

```
spatial.plot(G1, mur_coords$long, mur_coords$lat,
mur_coords$Object.ID, xlab = "Longitude", ylab = "Latitude", plot.dry
= TRUE, col = "orange", pt.bg = "skyblue")
```

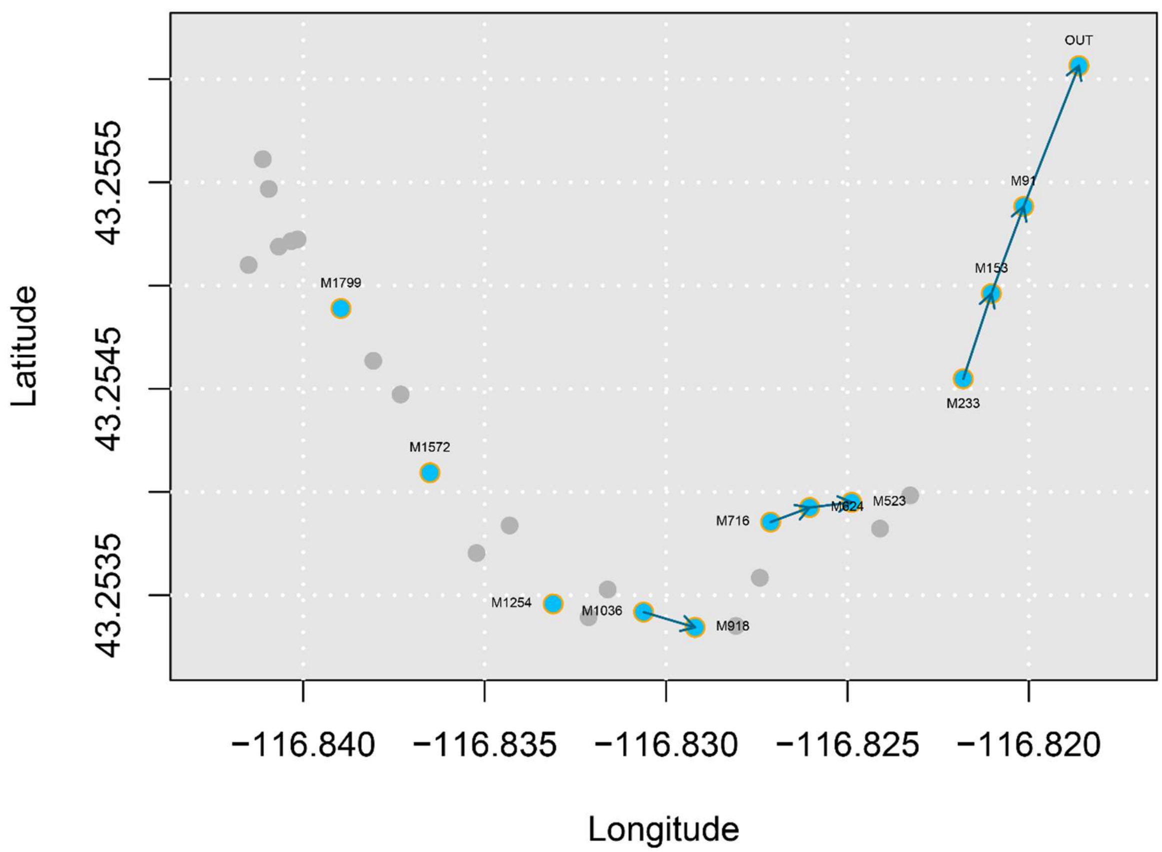

Figure 4. Wet nodes and deduced wet arcs (blue) are distinguished from dry nodes (gray) at Murphy Creek for the timestamp: 8/9/2019 22:30. Modification of the `murphy_spring` complete network object was accomplished using the function `delete.nodes.pa()`.

4.5 Unweighted DAG measures

A large number of local unweighted DAG metrics can be obtained from the *streamDAG* function `local.summary()`. Figure 5 summarizes nodal results for the complete Konza Prairie network (Fig 3b). Along the *x*-axis, nodes are ordered roughly from sources (leftmost nine nodes) to the sink (rightmost node). The importance of nodes at reach convergence points, e.g., SFM02_1, and the catchment outlet, e.g., SFM01_1, is evident. Note that metrics generally indicate an increase in nodal importance as distance to the sink decreases. An exception is betweenness centrality which is highest for nodes in the center of reaches, but lowest for the source and sink nodes.

```
local <- local.summary(streamDAGs("konza_full"))
barplot(t(scale(t(local)[,c(1,2,3,4,9)])), beside = T, las = 2)
```

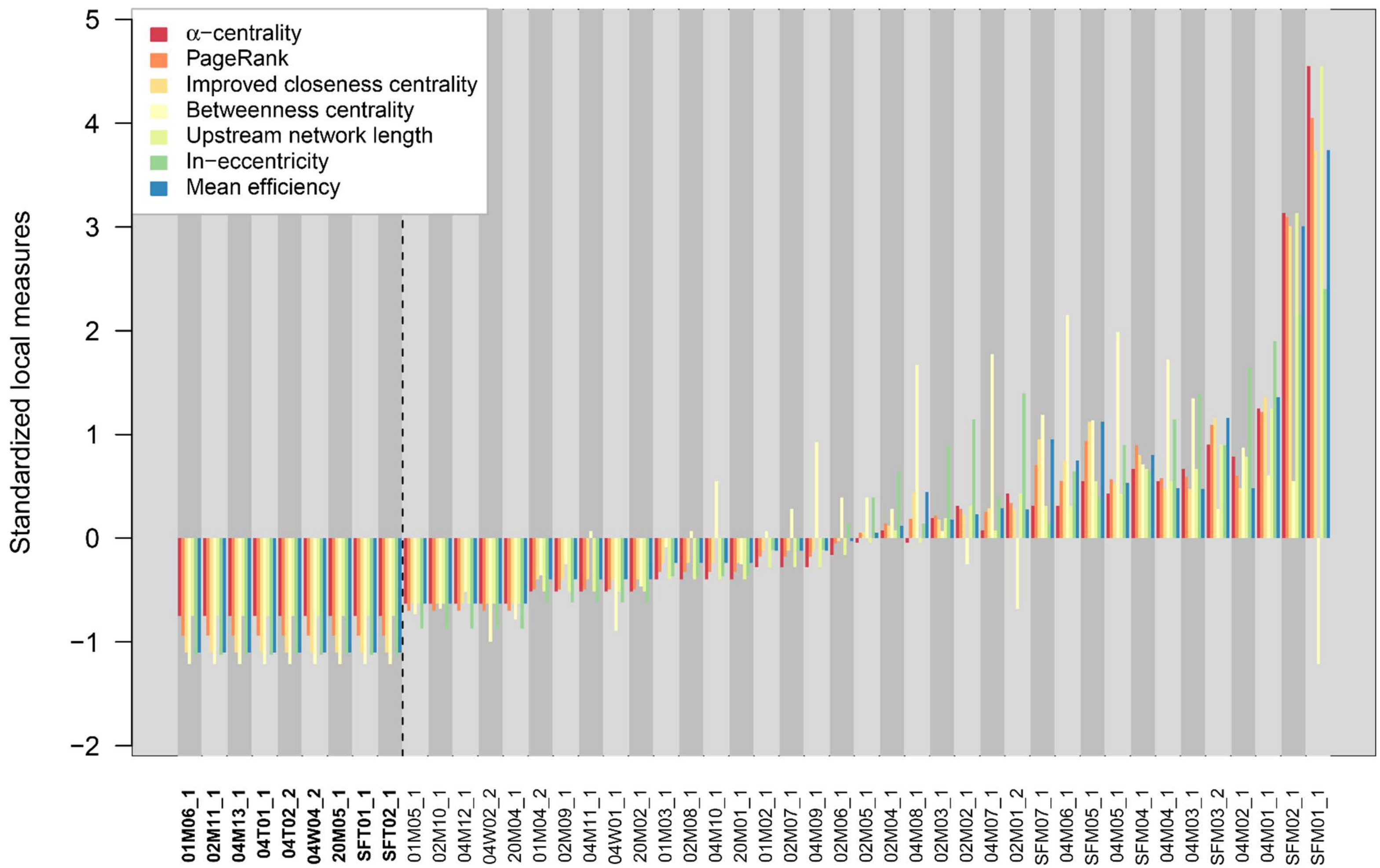

Figure 5. Local graph-theoretic summaries for the fully wetted Konza Prairie network using `local.summary()`. Metrics are standardized so that each has mean of zero and unit variance. Nodes are organized along the *x*-axis from sources to outlet using the ordering approach for visibilities applied in Fig. 6. A dashed line separates sources node from other nodes, and source IDs are bolded. Figure code can be found in Appendix B.

Nodal visibilities, based by default on node indegree, can be obtained with the function `multi.path.visibility()`. Ordering of nodes, vitally important to the calculation of visibility is currently accomplished by identifying paths from each source node to the sink. The sum of node distances in each path are then sorted decreasingly to define an initial order for calculating visibilities. As of *streamDAG* version 1.2-7, it is assumed that the user will manually handle disconnected paths via the `source` argument in visibility functions.

Visibility analysis of the complete Konza network strongly emphasizes the importance of the sink node SFM01_1 at the catchment outlet (Fig 6). Specifically, the relatively high indegree of SFM01_1 and its relative isolation from other high degree nodes, particularly along the westernmost reach (Fig 3B), allow this node to "see", or "be seen by" many upstream nodes in the network. Downstream visibilities of SFM01_1 are zero because it is the network outlet (Fig 6).

```
vis <- multi.path.visibility(murphy_spring, source = c("IN_N","IN_S"),
sink = "OUT")
barplot(vis$visibility.summary, las = 2, ylab = "Visible nodes")
```

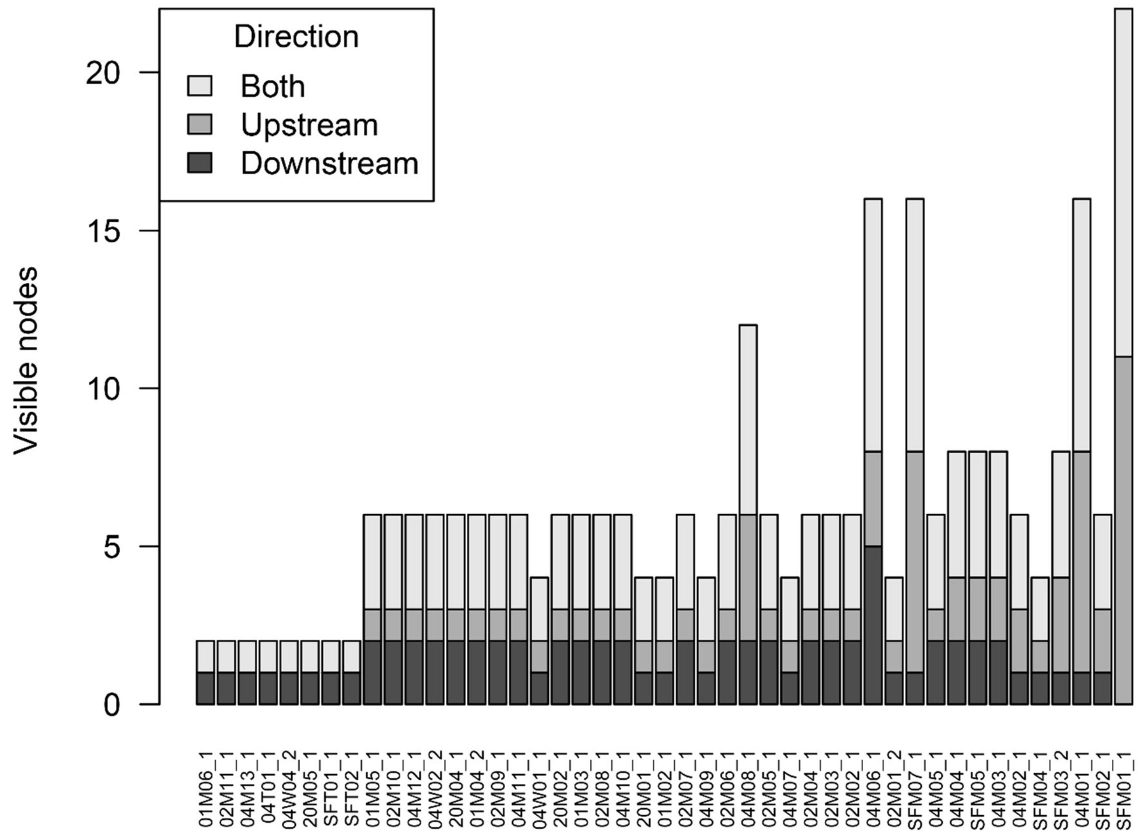

Figure 6: Nodal visibilities for the complete Konza Prairie network, based on nodal indegree. Nodes are organized approximately along the *x*-axis from sources to outlet.

A large number of global metrics are available from the *streamDAG* function `global.summary()`. Below we see comparisons of global metrics for the complete Murphy Creek and complete Konza Prairie networks that clearly illustrate the greater complexity of the Konza network by larger values for all metrics except mean upstream in-path length and mean α-centrality. These latter values reflect differences in node definitions, basin size, and density of sensor placement.

```
mur_global <- global.summary(streamDAGs("mur_full"), sink = "OUT")

kon_global <- global.summary(streamDAGs("konza_full"), "SFM01_1")

cbind(mur_global, kon_global)

                           Murphy        Konza

Size                     27.00000000    45.00000000
```

Diameter	25.00000000	14.00000000
Sources	2.00000000	9.00000000
n.paths.to.sink	27.00000000	45.00000000
mean.path.length	13.77777778	6.51111111
mean.a.centrality	14.28571429	7.36956522
Strahler.number	2.00000000	3.00000000
Shreve.number	2.00000000	9.00000000
Randic	13.20710678	20.15685425
first.Zagreb	28.00000000	53.00000000
second.Zagreb	14.50000000	30.50000000
ABC	0.70710678	5.65685425
Geom.Arith	13.44280904	22.04247233
Harmonic	13.16666667	19.83333333
Harary	40.86258116	53.89189422
Global.efficiency	0.10810207	0.05206946
Assort.in.out	-0.02192645	-0.19746510
Assort.in.in	0.03162278	0.05551808

It may be informative to track changes in global metrics (and local metrics) over time. Figure 7 shows a 100-point time series that spans the entire 2019 sampling season at Murphy Creek (completely wetted network shown in Fig 3b). Over this period, graphs were created to reflect presence or absence of water at Murphy Creek nodes, and global metrics were calculated from these graphs. Note that higher scores, indicating higher network connectivity, occur for most metrics during the spring and a re-wet period during the fall. An exception is in-out assortativity, $r(-,+)$, which increases during the drying period due to increasing homogenization of graph characteristics.

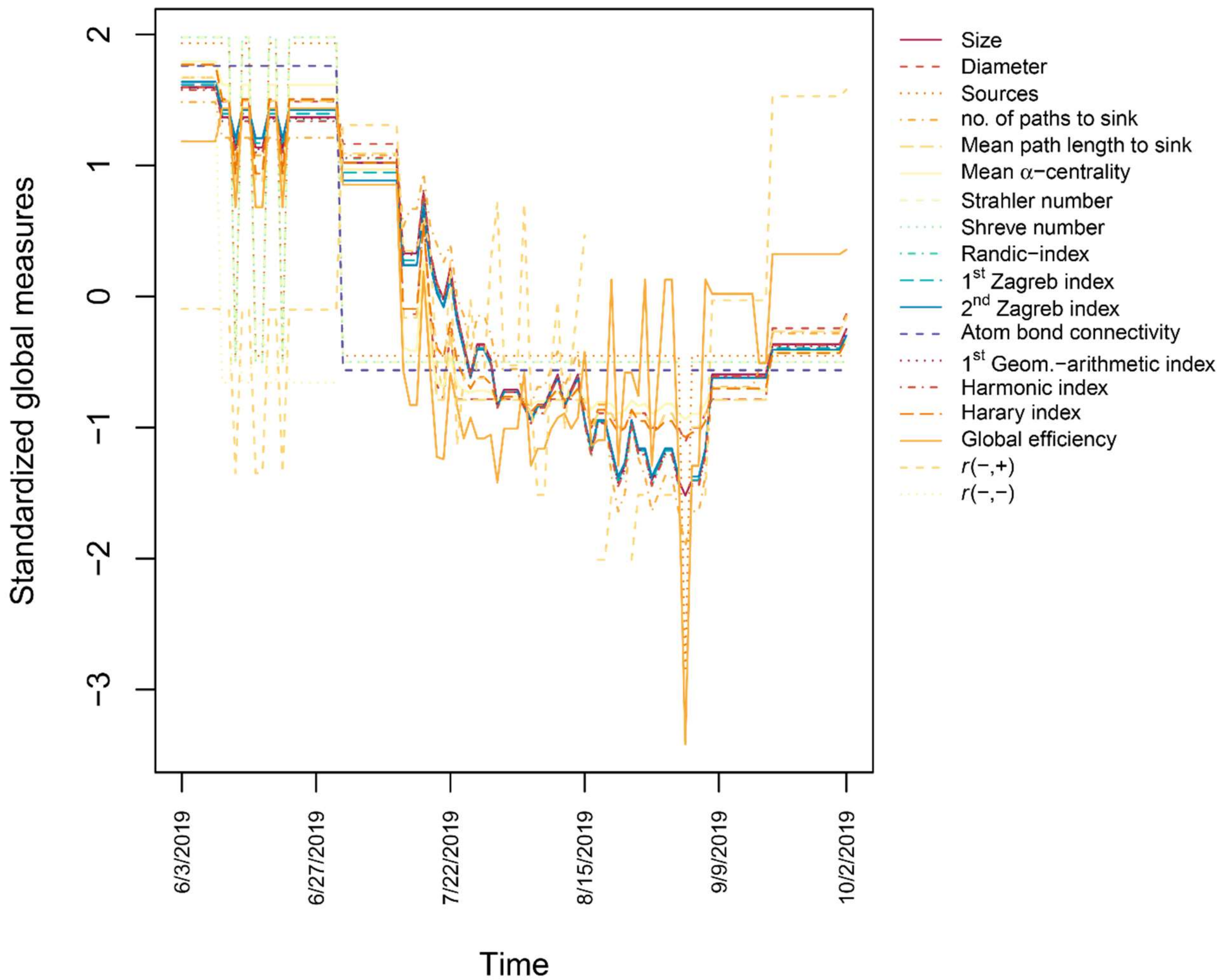

Figure 7. Global complexity, connectivity, and assortativity summaries for Murphy Creek based on stream node presence / absence data. As in Fig 6, metrics are standardized to have a mean of zero and unit variance. Figure code can be found in Appendix B.

4.7 Weighted DAG measures

Realism in descriptions of non-perennial stream DAGs can be enhanced by using relevant weighting information. Fig 8 shows two weighted local arc-based summaries: mean Bernoulli stream length and mean communication distance based on surface water presence/absence data from Murphy Creek in 2019. Note the large communication distance for $\overrightarrow{INS\ M1993}$, indicating a high propensity for stream bottlenecks at this arc.

```
prob <- colMeans(mur_arc_pres_abs)
```

```
bsl <- bern.length(mur_lengths[,2], prob) # Bernoulli length

bcd <- bern.length(mur_lengths[,2], 1/prob) # Comm dist.

barplot(t(scale(cbind(bsl, bcd))), beside = T, las = 2)
```

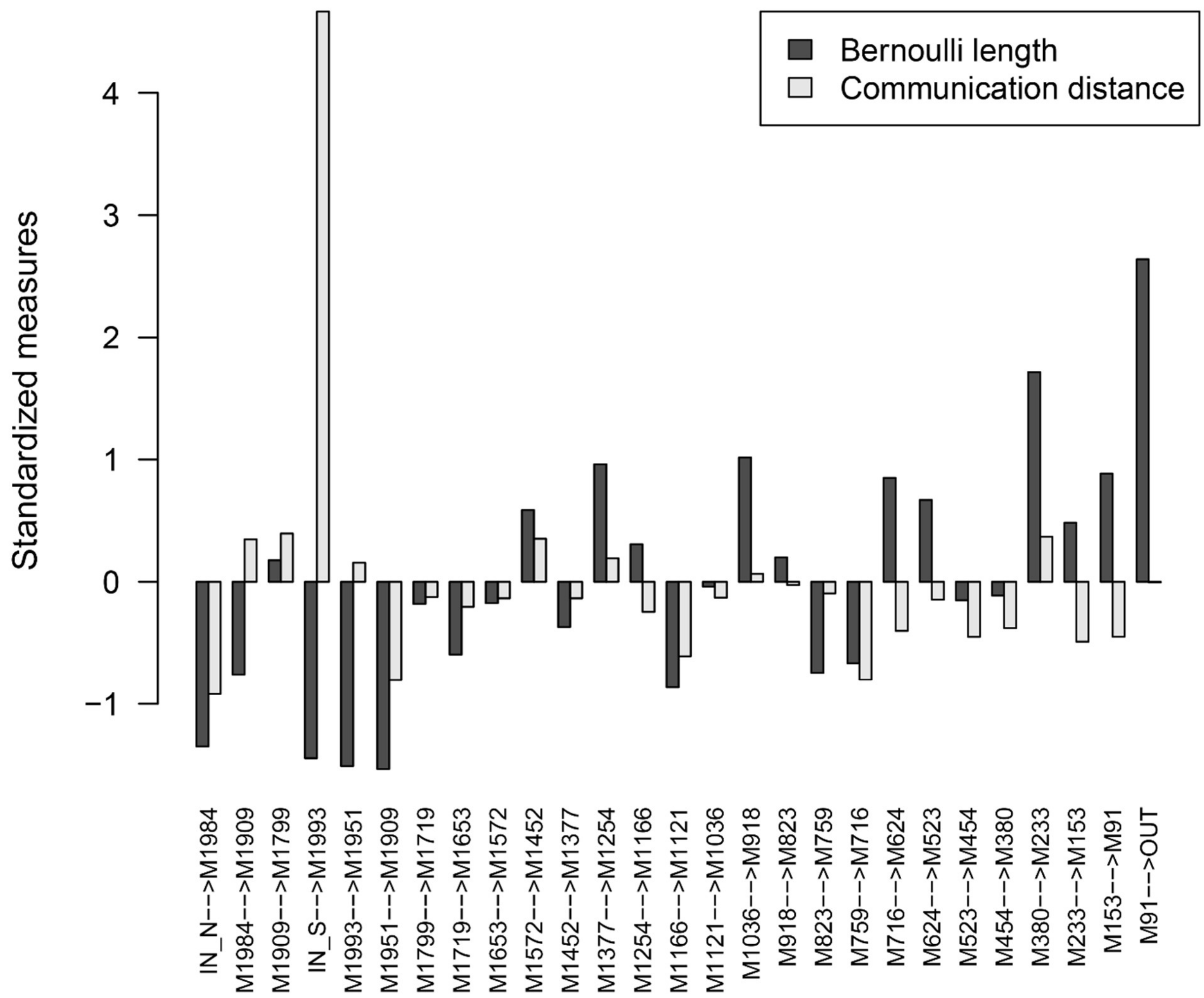

Fig. 8 Bernoulli length and communication distance using stream segment length and stream segment probability of surface water presence together as arc weights. Code for creating the figure can be found in Appendix B.

As with unweighted metrics, it may be informative to track weighted global (and local) metrics for non-perennial streams over time. In Fig 9, we consider the weighted global metrics ICSL, intact stream length to the node, and average alpha-centrality (with instream lengths as arc weights) for Murphy Creek graphs over time, based on the stream node time series data in Fig 7. All three metrics show dramatic decreases in network connectivity from spring to summer, with a connectivity uptick in the fall (Fig 9).

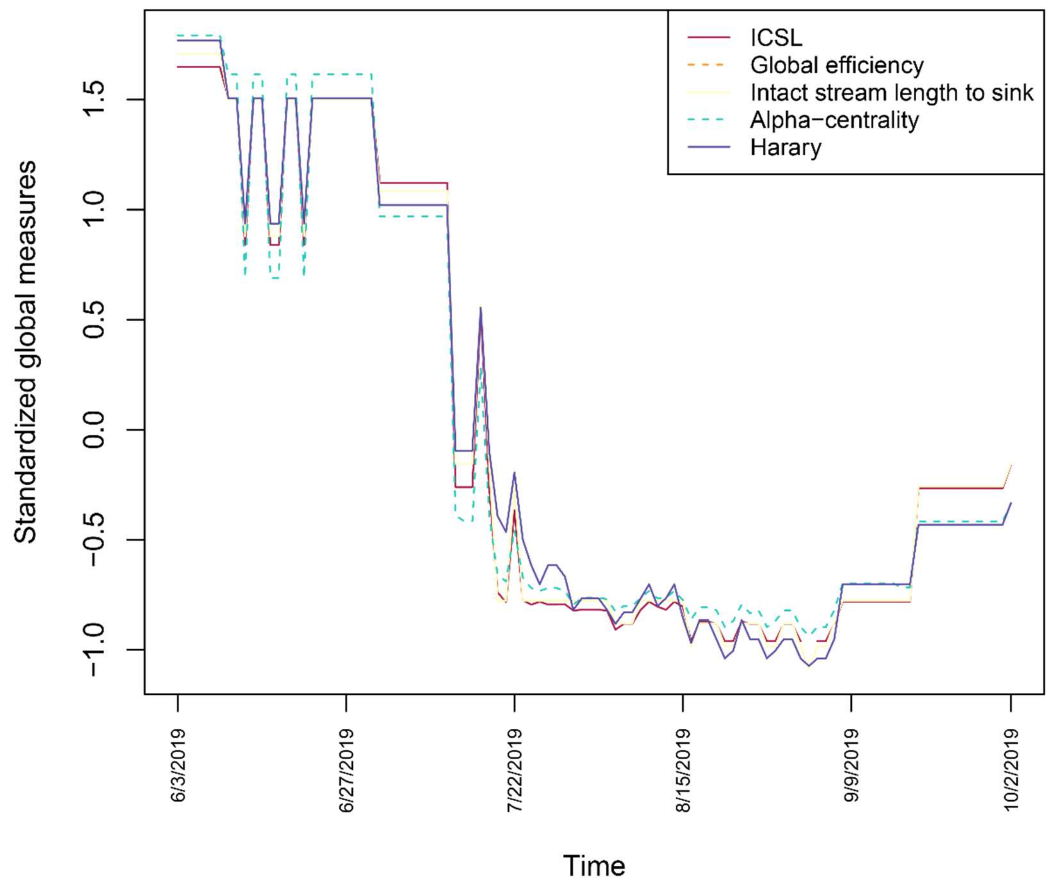

Figure 9. Global weighted (by arc instream lengths) network connectivity measures for Murphy Creek over time. Code for creating the figure can be found in Appendix B.

4.8 Bayesian applications

Bayesian analyses using Bernoulli stream length and communication distance are facilitated by use of the *streamDAG* function `beta.posterior()`. As an example, assume that we wish to apply a naive Bayesian prior, $\theta_k \sim BETA(1,1)$, for the probability of stream segment surface water presence at Murphy Creek, to all stream segments. Note that the distribution $BETA(1,1)$ is equivalent to a continuous uniform distribution in 0,1, and will have mean, $E(\theta) = 0.5$. Assume further that we wish to give the priors 1/3 of the weight of observed binomial data outcomes (i.e., stream presence observations over *n* trials). The `mur_arc_pres_abs` dataframe contains 1000 simulated multivariate Bernoulli datasets for Murphy Creek, one per row. For demonstration purposes we will arbitrarily use the first 10 rows of the matrix `mur_arc_pres_abs` as an observed multivariate binomial data point. We have:

```
data <- mur_arc_pres_abs[1:10,]

b <- beta.posterior(p.prior = 0.5, dat = data, length =
mur_lengths[,2], w = 1/3)
```

The function `beta.posterior()` returns a list with values for shape parameters for the beta posteriors for the probability of stream presence (Fig. 10) and the inverse beta parameters for the reciprocal probability of stream presence.

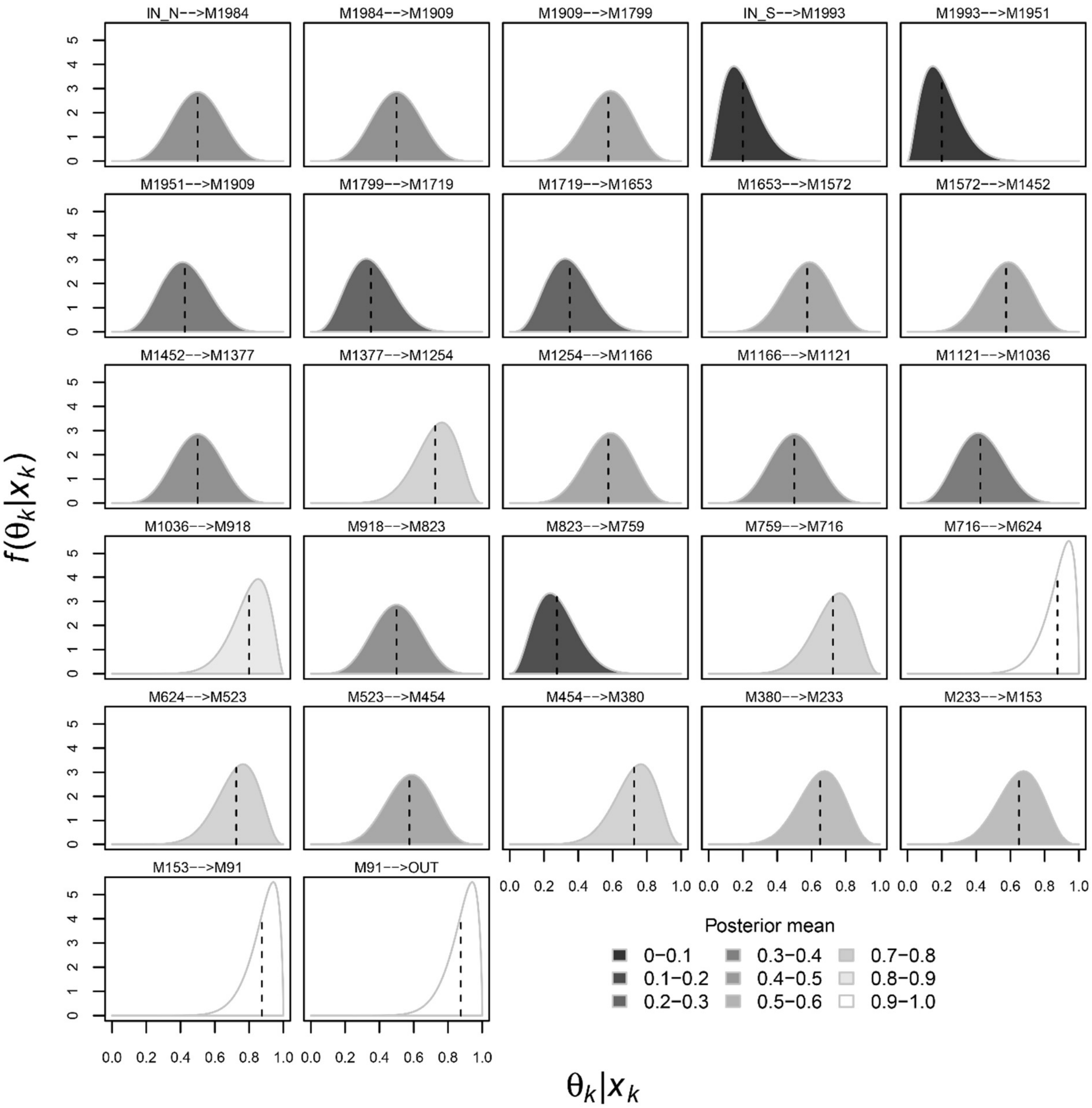

Figure 10. Graphical summaries of posterior beta distributions representing the probabilities of stream surface water for Murphy Creek stream arcs from 06/01/2019 to 10/01/2019. Arc distributions are colored by their mean values (darker distributions have smaller means). Posterior means are overlain on the distributions with dashed lines. Code for creating the figure can be found in Appendix B.

5. Discussion

The spatiotemporal variability of non-perennial streams is often not well represented by common metrics of stream network complexity and connectivity, many of which are time invariant. Further, many existing stream metrics do not consider the importance of individual stream locations to stream network functionality and stability. This deficiency is particularly problematic in non-perennial streams because certain stream locations (e.g., bottlenecks) may have inordinately large effects on the entire networks. Moreover, many stream functions, particularly those involving biogeochemical processes, may asynchronous with hydrological connectivity (Stevenson and Sabater 2015; Jensen et al. 2019; Jiang et al, 2020; Niyogi et al., 2020; Shanafield et al., 2021; Sarremejane et al., 2022). Therefore, connectivity assessments based purely on non-perennial stream water presence / absence snapshots may not serve as adequate predictors for many stream processes.

Our proposed alternative is to view non-perennial streams as directed acyclic graphs (DAGs). Our approach allows standardized graphical and numeric tracking of global stream network characteristics as streams dry, and consideration of the importance of both local stream components (e.g. arcs and nodes) to overall network function, and global network characteristics. Specifically, DAG metrics allow 1) quantification of the centrality, connectedness, and nestedness of nodes, arcs and entire networks, and 2) tracking of these characteristics as non-perennial stream networks expand and shrink. In our work we consider a large number of graph theoretic methods that are potentially useful to the analysis of stream DAGs, and further, in Appendix A, identify methods that are *unlikely* to be useful. We deem the latter contribution helpful given the confusing myriad of graph theoretic methods, many of which have been "rediscovered" under different names. See Phillips et al. (2015), for a broad consideration of graph theory in the geosciences.

5.1 The *streamDAG* package

Our package *streamDAG* allows *igraph* codification and modification of stream DAGs using non-perennial stream presence / absence data, and implementation of a wide variety of DAG-appropriate metrics including local and global measures for both unweighted and weighted graphs. The package also facilitates Bayesian extensions to the Bernoulli stream length and communication distance weighted metrics introduced in Aho et al. (2023).

We applied *streamDAG* algorithms to both Murphy Creek, a simple drainage system consisting of one singly branched path, and Konza Prairie, a relatively complex stream network with nine source nodes and three major reaches (Section 4). These analyses allowed objective differentiation of general stream network characteristics, and descriptions of spatiotemporal variation in connectivity and complexity. Previously, our research group found that conventional hydrological descriptors of stream connectivity based on wet/dry status, elevation, slope, and drainage area were poorly correlated with any measure of aquatic microbiome alpha diversity at Konza Prairie (manuscript *in prep*). We found, however, that nodal prokaryotic taxa richness and Shannon diversity in the water column were strongly positively correlated to a large number of simple nodal graph theoretic metrics available in *streamDAG* including alpha centrality, improved closeness centrality, path number, mean path length, path length variance, in-eccentricity, and Shreve stream order (Fig 11). Aho et al. (2023) also obtained useful Bayesian summaries of connectivity at Murphy Creek using *streamDAG* functions for Bernoulli stream length and communication distance. We are hopeful that the usefulness of *streamDAG* functions observed at Konza Prairie and Murphy Creek will be extendable to non-perennial streams elsewhere.

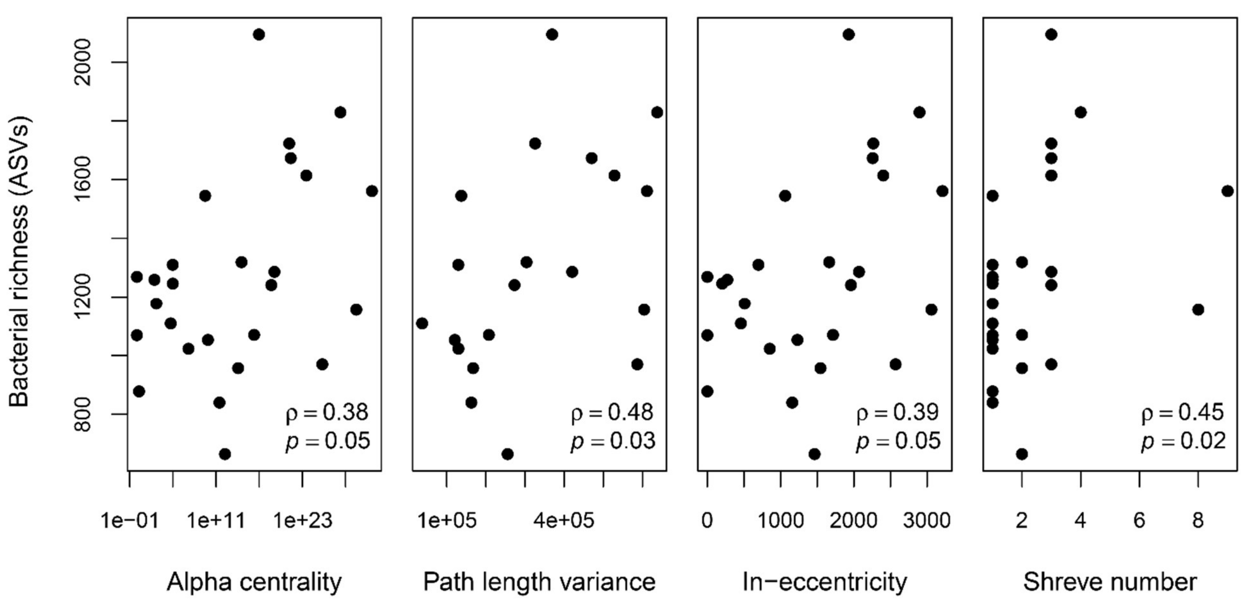

Figure 11. Associations of Konza Prairie water column prokaryotic taxa richness (i.e., amplicon sequence variants (ASVs) identified sing 16S genetic sequencing) and four measures of nodal

importance and connectivity (n = 26) at Konza Prairie. Numbers in the bottom right of each plot are the Spearman's correlations (rho) and resulting p-values for the null hypothesis of independence. Alpha centrality, path length variance and in-eccentricity were based on arcs weighted by actually in-stream lengths.

5.1.1 Comparisons of streamDAG to existing software. The goal of describing stream network characteristics, including network connectivity, has driven the development of several computer algorithms and software packages. These include the **R** packages *rtop* (Skøien et al. 2012), *SSN* (ver Hoef et al. 2014), *riverconn* (Baldan et al. 2022), and *streamDepletr* (Zipper 2020), and the *geostatistical connectivity* algorithm of Pardo-Igúzquiza and Dowd (2003) originally written in FORTRAN, and later codified in MATLAB (Trigg et al. 2013). The *streamDAG* package can be distinguished from these efforts in at least two ways.

First, *streamDAG* algorithms codify graph theoretic metrics relevant to non-perennial streams (e.g., the Harary index, $I(D)$ metrics) in addition to existing surficial hydrological measures (e.g., stream order, ICSL, Bernoulli stream length). In contrast, the *riverconn* package considers existing organismal dispersal connectivity metrics, with the potential for bidirectional (non-DAG) arcs, and with nodes as reaches and arcs as barriers or connections or splits rather than arcs as stream segments (Section 1.1). Although these methods are not codified in *streamDAG*, we briefly consider the *RCI* (Eq. 8) and *CCI* (Eq. 9) approaches used by *riverconn* in Section 3.2 and 3.3, respectively. Unlike *streamDAG*, the *SSN* package is not concerned with graph theory or hydrologic metrics, but with the development and application of stream-appropriate spatial covariance structures, including those of Cressie et al. (2006) and Ver Hoef et al. (2006), to allow the extension of conventional spatial statistical models to streams. The *SSN* framework has been expanded by other authors to include, among other applications, Bayesian generalized linear models (the *SSNbayes* **R** package; Santos-Fernandez et al. 2022). The package *rtop* (Skøien et al. 2012) uses covariance approaches other than those in *SSN* (see Skøien et al. 2006) for the same purpose: to produce stream network spatial models. The focus of *streamDAG* on surface flow networks is also very different from *streamDepletr,* which estimates potential pumping impacts on streamflow based on inferred stream-aquifer connections (Zipper 2020).

Second, *streamDAG* maintains a focus on non-perennial streams through functions capable of incorporating water presence/absence data at nodes and arcs. Conversely, *riverconn* connectivity metrics stress the importance of physical barriers to streamflow, particularly anthropogenic dams, which are unlikely to occur in non-perennial streams. The non-perennial focus of *streamDAG* is also distinct from the grid-reliant geostatistical connectivity algorithm (Pardo-Igúzquiza and Dowd 2003), which lends itself to analysis of remotely sensed floodplain images based on continuous grids (see Trigg et al. 2013, Karim et al. 2015, Chen et al. 2020).

5.2 Correlations of graph-theory measures

We observed varying but often strong correspondence in the assessments of local and global metrics in the analyses of both artificial stream graphs (Fig. 2), and the Konza Prairie and Murphy Creek networks (Figs. 5, 7, 8, 9). The correlation of local centrality measures (e.g., closeness centrality, degree, eigenvector centrality, betweenness centrality) has been considered previously (e.g., Valente 2008, Batool and Niazi 2014, Li et al. 2015). These papers often hold that correlations of centrality measures are due to similarities in the formal definitions of indices and that an absence of correlations between indices is due to divergent conceptualizations of centrality (Schoch et al. 2017). However, inconsistencies in some empirical findings and a re-consideration of graphs with respect to their *neighborhood inclusion preorder* indicate that underlying directed network structures may strongly affect the strength of correlations among local centrality measures (see Schoch et al. 2017). Empirical assessments of the correlation of global graph measures are largely lacking, although relevant ancillary summaries are given in a number of papers including Foo et al. (2021).

5.3 Uncertainties and extensions

Our work considers surficial stream networks. In principle one could consider both subsurface networks (although network structure specifications may be particularly challenging. given fundamental differences between surface water channels and groundwatersheds; Huggins et al., (2022)), and subsurface to surface hydrologic fluxes (e.g., vertical connectivity) from a graph theory perspective. Stream vertical connectivity has received less attention from hydrologists compared to surficial connectivity due to the increased difficulty in obtaining subsurface permeability and flowpath information (Xiao et al. 2021). While potentially useful, models of vertical connectivity, based on subsurface reactive transport algorithms (Steefel et al. 2015), and hillslope models (Hopp and McDonnell 2009), remain largely limited to time invariant perspectives (Xiao et al. 2021).

Finally, we note that stream DAG nodes and resultant arcs will be user-defined, causing discrepancies in their designation to strongly affect stream network topology. As a result, node locations in a stream graph should be consistent and/or hydrologically meaningful. For instance, nodes could represent approximately equidistant points along stream paths and/or joins, splits, sinks, or sources. The effect of biased or otherwise sub-optimal node designations can be moderated by applying reality-driven weights to arcs or nodes. For instance, graph-theoretic in-path lengths for a node, v, can be made arbitrarily large by simply adding more nodes to paths ending in v. This undesirable effect, however, can be assuaged if arcs are weighted by their actual field-measured lengths. Weighted graph approaches also allow the incorporation of both structural (topological) and functional perspectives when describing streams (Baldan et al. 2022). Thus, these measures may be superior to unweighted approaches when considering node-specific information unrelated to topology.

6. Acknowledgements

This work was made possible with a grant from the National Science Foundation RII Track-2 FEC: Aquatic Intermittency Effects on Microbiomes in Streams (AIMS) (NSF award 2019603) and NSF EAR1653998. Special thanks to Arya Legg for codifying documentation files for *streamDAG*, and the broader AIMS research group for their commentary and ideas as the *streamDAG* package developed.

7. Bibliography

Aho, K. A. (2014). *Foundational and Applied Statistics for Biologists Using R*. CRC Press.

Aho et al. (2023). The Communication Distance of Non-perennial Streams. *EarthArXiv*

Albert, R., and Barabási, A. L. (2002). Statistical mechanics of complex networks. *Reviews of modern physics*, *74*(1), 47.

Ali, G. A., and Roy, A. G. (2009). Revisiting hydrologic sampling strategies for an accurate assessment of hydrologic connectivity in humid temperate systems. *Geography Compass*, *3*(1), 350–374.

Ali, G. A., and Roy, A. G. (2010). Shopping for hydrologically representative connectivity metrics in a humid temperate forested catchment. *Water Resources Research*, *46*(12).

Angulo-Rodeles, A., Galicia-Paredes, D., and Miranda, R. (2021). A simple method to assess the fragmentation of freshwater fish meta-populations: implications for river management and conservation. *Ecological Indicators* 125 107557

Anthony, B. M., and Marr, A. M. (2021). Directed Zagreb indices. *Graphs and Combinatorial Optimization: From Theory to Applications: Ctw2020 Proceedings*, 181–193.

Arizmendi, G., and Arizmendi, O. (2022). Energy and Randić index of directed graphs. *Linear and Multilinear Algebra*, 1-12.

Balaban, A. T. (1982). Highly discriminating distance-based topological index. *Chemical Physics Letters*, *89*(5), 399-404.

Baldan, D., Cunillera-Montcusí, D., Funk, A., and Hein, T. (2022). Riverconn: An R Package to Assess River Network Fragmentation. *Environmental Modelling and Software,* http://dx.doi.org/10.2139/ssrn.4096555 (verified 11/18/2022)

Bang-Jensen, J., & Gutin, G. (2007). Digraghs: Theory, algorithms and applications. *Springer Monographs in Mathematics, Springer-Verlag London Ltd., London*, *101*.

Barrat, A., Barthelemy, M., Pastor-Satorras, R., and Vespignani, A. (2004). The architecture of complex weighted networks. *Proceedings of the National Academy of Sciences*, *101*(11), 3747-3752.

Batool, K., and Niazi, M. A. (2014). Towards a methodology for validation of centrality measures in complex networks. *PloS one, 9*(4), e90283.

Beauchamp, M. A. (1965). An improved index of centrality. *Behavioral Science*, *10*(2), 161–163.

Beven, K. J., and Kirkby, M. J. (1979). A physically based, variable contributing area model of basin hydrology/un modèle à base physique de zone d'appel variable de l'hydrologie du bassin versant. *Hydrological Sciences Journal*, *24*(1), 43–69.

Bhanumathi, M., and Rani, K. E. J. (2018). On multilplicative sum connectivity index, multilplicative Randić index and multilplicative harmonic index of some nanostar dendrimers. *International Journal of Engineering Science, Advanced Computing and Bio-Technology*, *9*(2), 52–67.

Bonacich, P. (1972). Factoring and weighting approaches to status scores and clique identification. *Journal of Mathematical Sociology*, *2*(1), 113-120.

Bonacich, P. (1987). Power and centrality: A family of measures. *American Journal of Sociology*, *92*(5), 1170-1182.

Bonacich, P., and Lloyd, P. (2001). Eigenvector-like measures of centrality for asymmetric relations. *Social Networks*, 23(3), 191-201.

Borgatti, S. P. (2005). Centrality and network flow. *Social Networks*, *27*(1), 55–71.

Borgatti, S. P., & Everett, M. G. (2006). A graph-theoretic perspective on centrality. *Social networks*, *28*(4), 466-484.

Borselli, L., Cassi, P., and Torri, D. (2008). Prolegomena to sediment and flow connectivity in the landscape: a GIS and field numerical assessment. *Catena*, *75*(3), 268-277.

Botter, G., and Durighetto, N. (2020). The stream length duration curve: A tool for characterizing the time variability of the flowing stream length. *Water Resources Research*, *56*(8), e2020WR027282.

Bozovic, V., Vukicevic, Z. K., and Popivoda, G. (2016). Chemical trees with extreme values of a few types of multiplicative Zagreb indices. *MATCH Commun. Math. Comput. Chem*, *76*, 207–220.

Bracken, L., Wainwright, J., Ali, G., Tetzlaff, D., Smith, M., Reaney, S., and Roy, A. (2013). Concepts of hydrological connectivity: Research approaches, pathways and future agendas. *Earth-Science Reviews*, *119*, 17–34.

Brandes, U., and Fleischer, D. (2005). Centrality measures based on current flow. In *Annual symposium on theoretical aspects of computer science* (pp. 533-544). Springer, Berlin, Heidelberg.

Chen, Y., Wu, L., Zhang, G., Xu, Y. J., Tan, Z., and Qiao, S. (2020). Assessment of surface hydrological connectivity in an ungauged multi-lake system with a combined approach using geostatistics and spaceborne SAR observations. *Water*, *12*(10), 2780.

Cote, D., Kehler, D. G., Bourne, C., and Wiersma, Y. F. (2009). A new measure of longitudinal connectivity for stream networks. *Landscape Ecology*, 24(1), 101-113.

Csardi, G., and Nepusz, T. (2006). The igraph software package for complex network research. *InterJournal*, *Complex Systems*, 1695.

Das, K. C., Gutman, I., and Furtula, B. (2011). On atom-bond connectivity index. *Chemical Physics Letters*, *511*(4-6), 452–454.

Dekker, A. (2005). Conceptual distance in social network analysis. *Journal of Social Structure*, *6*(3), 31.

Deng, H., Yang, J., Tang, Z., Yang, J., and You, M. (2022). On the vertex-degree based invariants of digraphs. *Discrete Math. Lett. 9,* 2–9.

Dodds, P. S., and Rothman, D. H. (2000). Geometry of river networks. I. Scaling, fluctuations, and deviations. *Physical Review E*, *63*(1), 016115.

Durighetto, N., and Botter, G. (2022). On the relation between active network length and catchment discharge. *Geophysical Research Letters*, *49*(14), e2022GL099500.

Eliasi, M., and Ghalavand, A. (2016). Ordering of trees by multiplicative second zagreb index. *Transactions on Combinatorics*, *5*(1), 49–55.

Ek, B., VerSchneider, C., & Narayan, D. A. (2015). Global efficiency of graphs. *AKCE International Journal of Graphs and Combinatorics*, *12*(1), 1-13.

Estrada, E., Torres, L., Rodriguez, L., and Gutman, I. (1998). *An atom-bond connectivity index: Modelling the enthalpy of formation of alkanes*. NISCAIR-CSIR, India.

Favaron, O., Mahéo, M., and Saclé, J.-F. (1993). Some eigenvalue properties in graphs (conjectures of graffiti—II). *Discrete Mathematics*, *111*(1-3), 197–220.

Foo, H., Thalamuthu, A., Jiang, J., Koch, F., Mather, K. A., Wen, W., and Sachdev, P. S. (2021). Age-and sex-related topological organization of human brain functional networks and their relationship to cognition. *Frontiers in aging neuroscience*, 897.

Foster, J. G., Foster, D. V., Grassberger, P., and Paczuski, M. (2010). Edge direction and the structure of networks. *Proceedings of the National Academy of Sciences*, *107*(24), 10815–10820.

Freeman, L. C. (1977). A set of measures of centrality based on betweenness. *Sociometry*, 35-41.

Freeman, M. C., Pringle, C. M., and Jackson, C. R. (2007). Hydrologic connectivity and the contribution of stream headwaters to ecological integrity at regional scales 1. *JAWRA Journal of the American Water Resources Association*, *43*(1), 5–14.

Girvan, M., and Newman, M. E. (2002). Community structure in social and biological networks. *Proceedings of the National Academy of Sciences*, *99*(12), 7821-7826.

Godsey, S. E., & Kirchner, J. W. (2014). Dynamic, discontinuous stream networks: hydrologically driven variations in active drainage density, flowing channels and stream order. *Hydrological Processes*, *28*(23), 5791-5803.

Grill, G., Dallaire, C. O., Chouinard, E. F., Sindorf, N., and Lehner, B. (2014). Development of new indicators to evaluate river fragmentation and flow regulation at large scales: A case study for the Mekong River Basin. *Ecological Indicators*, 45, 148-159.

Gutman, I., Ruscić, B., Trinajstić, N., and Wilcox Jr, C. F. (1975). Graph theory and molecular orbitals. XII. Acyclic polyenes. *The Journal of Chemical Physics*, *62*(9), 3399-3405.

Gutman, I., Furtula, B., and Katanić, V. (2018). Randić index and information. *AKCE International Journal of Graphs and Combinatorics*, *15*(3), 307–312.

Harary, F., and Norman, R. Z. (1960). Some properties of line digraphs. *Rendiconti del Circolo Matematico di Palermo*, *9*(2), 161-168.

Hopp, L., and McDonnell, J. J. (2009). Connectivity at the hillslope scale: Identifying interactions between storm size, bedrock permeability, slope angle and soil depth. *Journal of Hydrology, 376*(3-4), 378-391.

Huggins, X., Gleeson, T., Serrano, D., Zipper, S., Jehn, F., Rohde, M.M., Abell, R., Vigerstol, K., Hartmann, A., 2022. Groundwatersheds of protected areas reveal globally overlooked risks and opportunities. *EarthArXiv.*

Igraph - The network analysis package. 2022. https://igraph.org/ (verified 11/18/2022)

Jencso, K. G., McGlynn, B. L., Gooseff, M. N., Wondzell, S. M., Bencala, K. E., and Marshall, L. A. (2009). Hydrologic connectivity between landscapes and streams: Transferring reach-and plot-scale understanding to the catchment scale. *Water Resources Research*, *45*(4).

Jia, X., Zwart, J., Sadler, J., Appling, A., Oliver, S., Markstrom, S., ... and Kumar, V. (2021). Physics-guided recurrent graph model for predicting flow and temperature in river networks. In Proceedings of the 2021 SIAM International Conference on Data Mining (SDM) (pp. 612-620). *Society for Industrial and Applied Mathematics*.

Karim, F., Dutta, D., Marvanek, S., Petheram, C., Ticehurst, C., Lerat, J., ... and Yang, A. (2015). Assessing the impacts of climate change and dams on floodplain inundation and wetland connectivity in the wet–dry tropics of northern Australia. *Journal of Hydrology*, *522*, 80-94.

Karrer, B., and Newman, M. E. (2009). Random graph models for directed acyclic networks. *Physical Review E*, *80*(4), 046110.

Katz, L. (1953). A new status index derived from sociometric analysis. *Psychometrika*, *18*(1), 39-43.

Kincaid, R. K., Kunkler, S. J., Lamar, M. D., and Phillips, D. J. (2016). Algorithms and complexity results for finding graphs with extremal Randić index. *Networks*, *67*(4), 338–347.

Kleinberg, J. M. (1999). Hubs, authorities, and communities. *ACM computing surveys (CSUR)*, *31*(4es), 5-es.

Knudby, C., and Carrera, J. (2005). On the relationship between indicators of geostatistical, flow and transport connectivity. *Advances in Water Resources*, 28(4), 405-421.

Krabbenhoft, C.A., Allen, G.H., Lin, P., Godsey, S.E., Allen, D.C., Burrows, R.M., DelVecchia, A.G., Fritz, K.M., Shanafield, M., Burgin, A.J., Zimmer, M.A., Datry, T., Dodds, W.K., Jones, C.N., Mims, M.C., Franklin, C., Hammond, J.C., Zipper, S., Ward, A.S., Costigan, K.H., Beck, H.E., Olden, J.D., 2022. Assessing placement bias of the global river gauge network. *Nature Sustainability*, 1–7. https://doi.org/10.1038/s41893-022-00873-0

Lacasa, L., Luque, B., Ballesteros, F., Luque, J., and Nuno, J. C. (2008). From time series to complex networks: The visibility graph. *Proceedings of the National Academy of Sciences*, *105*(13), 4972-4975.

Lacasa, L., and Toral, R. (2010). Description of stochastic and chaotic series using visibility graphs. *Physical Review E*, *82*(3), 036120.

Lane, S. N. Reaney, S. M. et al. 2009. Representation of landscape hydrological connectivity using a topographically driven surface flow index. *Water Resources Research*, 45(8).

Larsen, L. G., Choi, J., Nungesser, M. K., and Harvey, J. W. (2012). Directional connectivity in hydrology and ecology. *Ecological Applications*, *22*(8), 2204–2220.

Latora, V., & Marchiori, M. (2001). Efficient behavior of small-world networks. *Physical Review Letters*, *87*(19), 198701.

Li, C., Li, Q., Van Mieghem, P., Stanley, H. E., and Wang, H. (2015). Correlation between centrality metrics and their application to the opinion model. *The European Physical Journal B*, *88*(3), 1-13.

Li, L., Alderson, D., Doyle, J. C., and Willinger, W. (2005). Towards a theory of scale-free graphs: Definition, properties, and implications. *Internet Mathematics*, *2*(4), 431-523.

Li, X., and Shi, Y. (2008). A survey on the Randić index. *MATCH Commun. Math. Comput. Chem*, *59*(1), 127–156.

Liu, Y., Hou, G., Huang, F., Qin, H., Wang, B., and Yi, L. (2022). Directed Graph Deep Neural Network for Multi-step Daily Streamflow Forecasting. *Journal of Hydrology*, 127515.

Luque, B., Lacasa, L., Ballesteros, F., and Luque, J. (2009). Horizontal visibility graphs: Exact results for random time series. *Physical Review E*, *80*(4), 046103.

Maidment, D. R. (1996). GIS and hydrologic modeling-an assessment of progress. In *Third International Conference on GIS and Environmental Modeling, Santa Fe, New Mexico*.

Monsalve, J., and Rada, J. (2021a). Vertex-degree based topological indices of digraphs. *Discrete Applied Mathematics*, *295*, 13–24.

Monsalve, J., and Rada, J. (2021b). Sharp upper and lower bounds of VDB topological indices of digraphs. *Symmetry*, *13*(10), 1903.

Newman, M. E. (2002). Assortative mixing in networks. *Physical Review Letters*, *89*(20), 208701.

Newman, M. E. (2005). A measure of betweenness centrality based on random walks. *Social Networks, 27*, 39-54.

Newman, M. E. (2006). Finding community structure in networks using the eigenvectors of matrices. *Physical review E*, *74*(3), 036104.

Newman, M. E. (2008). The mathematics of networks. *The New Palgrave Encyclopedia of Economics*, *2*(2008), 1–12.

Newman, M. E. (2018). *Networks, 2nd edition*. Oxford University Press.

Opsahl, T., Agneessens, F., and Skvoretz, J. (2010). Node centrality in weighted networks: Generalizing degree and shortest paths. *Social Networks*, 32(3), 245-251.

Pardo-Igúzquiza, E., and Dowd, P. A. (2003). CONNEC3D: a computer program for connectivity analysis of 3D random set models. *Computers and Geosciences*, *29*(6), 775-785.

Pascual-Hortal, L., and Saura, S. (2006). Comparison and development of new graph-based landscape connectivity indices: towards the priorization of habitat patches and corridors for conservation. *Landscape ecology, 21*(7), 959-967.

Phillips, J. D., Schwanghart, W., and Heckmann, T. (2015). Graph theory in the geosciences. *Earth-Science Reviews*, *143*, 147–160.

Plavšić, D., Nikolić, S., Trinajstić, N., and Mihalić, Z. (1993). On the Harary index for the characterization of chemical graphs. *Journal of Mathematical Chemistry*, *12*(1), 235–250.

R Core Team. (2021). *R: A language and environment for statistical computing*. R Foundation for Statistical Computing. https://www.R-project.org/ (verified 11/18/2022)

Randić, M. (1975). Characterization of molecular branching. *Journal of the American Chemical Society*, *97*(23), 6609-6615.

Randić, M. (1993). Novel molecular descriptor for structure—property studies. *Chemical Physics Letters*, *211*(4-5), 478-483.

Rochat, Y. 2009. Closeness centrality extended to unconnected graphs: The harmonic centrality index. *Applications of Social Network Analysis*, *ASNA*.

Rinaldo, A., Banavar, J. R., and Maritan, A. (2006). Trees, networks, and hydrology. *Water Resources Research*, *42*(6).

Santos-Fernandez, E., Ver Hoef, J. M., McGree, J. M., Isaak, D. J., Mengersen, K., Peterson, E. E. (2022). SSNbayes: An R package for Bayesian spatio-temporal modelling on stream networks. https://doi.org/10.48550/arXiv.2202.07166 (verified 11/18/2022)

Sarker, S., Veremyev, A., Boginski, V., and Singh, A. (2019). Critical nodes in river networks. *Scientific Reports*, *9*(1), 1–11.

Sarremejane, R., Messager, M.L. and Datry, T., 2022. Drought in intermittent river and ephemeral stream networks. *Ecohydrology, 15*(5), p.e2390.

Schoch, D., & Brandes, U. (2016). Re-conceptualizing centrality in social networks. *European Journal of Applied Mathematics*, *27*(6), 971-985.

Schoch, D., Valente, T. W., and Brandes, U. (2017). Correlations among centrality indices and a class of uniquely ranked graphs. *Social Networks*, *50*, 46-54.

Serinaldi, F., and Kilsby, C. G. (2016). Irreversibility and complex network behavior of stream flow fluctuations. *Physica A: Statistical Mechanics and its Applications*, 450, 585-600.

Shanafield, M., Bourke, S.A., Zimmer, M.A. and Costigan, K.H., 2021. An overview of the hydrology of non-perennial rivers and streams. Wiley Interdisciplinary Reviews: *Water, 8*(2), p.e1504.

Shannon, C. E. (1948). A mathematical theory of communication. *The Bell System Technical Journal*, *27*(3), 379-423.

Shreve, R. L. (1966). Statistical law of stream numbers. *The Journal of Geology*, *74*(1), 17-37.

Skøien, J. O., Merz, R., and Blöschl, G. (2006), Top-kriging-geostatistics on stream networks. *Hydrology and Earth System Sciences*, *10*(2), 277-287.

Skøien, J. O., Laaha, G., Koffler, D., Blöschl, G., Pebesma, E., Parajka, J. D., and Viglione, A. (2012), Rtop - an R package for interpolation along the stream network. In *Abstracts and Programme* (p. 1). *Geophysical Research Abstract*s. http://hdl.handle.net/20.500.12708/60971

Sørensen, R., Zinko, U., and Seibert, J. (2006). On the calculation of the topographic wetness index: evaluation of different methods based on field observations. *Hydrology and Earth System Sciences*, 10 (1): 101–112

Steefel, C. I., Appelo, C. A. J., Arora, B., Jacques, D., Kalbacher, T., Kolditz, O., ... and Yeh, G. T. (2015). Reactive transport codes for subsurface environmental simulation. *Computational Geosciences*, *19*(3), 445-478.

Strahler, A. N. (1957). Quantitative analysis of watershed geomorphology. *Eos, Transactions American Geophysical Union*, *38*(6), 913-920.

Trigg, M. A., Michaelides, K., Neal, J. C., and Bates, P. D. (2013). Surface water connectivity dynamics of a large-scale extreme flood. *Journal of Hydrology*, *505*, 138–149.

Valente, T. W., Coronges, K., Lakon, C., and Costenbader, E. (2008). How correlated are network centrality measures?. *Connections (Toronto, Ont.)*, *28*(1), 16.

Ver Hoef, J. M., Peterson, E., and Theobald, D. (2006). Spatial statistical models that use flow and stream distance. *Environmental and Ecological Statistics*, *13*(4), 449-464.

Ver Hoef, J., Peterson, E., Clifford, D., and Shah, R. (2014). SSN: An R package for spatial statistical modeling on stream networks. *Journal of Statistical Software*, *56*, 1-45.

Vukičević, D., and Furtula, B. (2009). Topological index based on the ratios of geometrical and arithmetical means of end-vertex degrees of edges. *Journal of Mathematical Chemistry*, *46*(4), 1369–1376.

Western, A.W., Blöschl, G., and Grayson, R.B. 2001. Toward capturing hydrologically significant connectivity in spatial patterns. *Water Resources Research*, 37 (1): 83-97

Xiao, D., Brantley, S. L., and Li, L. (2021). Vertical connectivity regulates water transit time and chemical weathering at the hillslope scale. *Water Resources Research*, *57*(8), e2020WR029207.

Zhong, L. (2012). The harmonic index for graphs. *Applied Mathematics Letters*, *25*(3), 561-566.

Zhou, B., and Trinajstić, N. (2009). On a novel connectivity index. *Journal of Mathematical Chemistry*, *46*(4), 1252–1270.

Zipper S (2020). *streamDepletr*: Estimate streamflow depletion due to groundwater pumping. R package version 0.1.1, https://CRAN.R-project.org/package=streamDepletr (verified 11/18/2022).